

Adaptive Riemannian Metrics on SPD Manifolds

Ziheng Chen¹ Yue Song¹ Tianyang Xu² Zhiwu Huang³ Xiao-Jun Wu² Nicu Sebe¹

Abstract

Symmetric Positive Definite (SPD) matrices have received wide attention in machine learning due to their intrinsic capacity of encoding underlying structural correlation in data. To reflect the non-Euclidean geometry of SPD manifolds, many successful Riemannian metrics have been proposed. However, existing fixed metric tensors might lead to sub-optimal performance for SPD matrices learning, especially for SPD neural networks. To remedy this limitation, we leverage the idea of pullback and propose adaptive Riemannian metrics for SPD manifolds. Moreover, we present comprehensive theories for our metrics. Experiments on three datasets demonstrate that equipped with the proposed metrics, SPD networks can exhibit superior performance.

1. Introduction

The Symmetric Positive Definite (SPD) matrices are ubiquitous in statistics, supporting a diversity of scientific areas, such as medical imaging (Chakraborty et al., 2018; 2020), signal processing (Arnaudon et al., 2013; Hua et al., 2017; Brooks et al., 2019b;a), elasticity (Moakher, 2006; Guilleminot & Soize, 2012), and computer vision (Huang & Van Gool, 2017; Harandi et al., 2018; Zhen et al., 2019; Chakraborty, 2020; Zhang et al., 2020; Chakraborty, 2020; Nguyen, 2021; 2022). Despite the exhibited capability of capturing data variations, SPD matrices cannot simply interact as points in a Euclidean space, which becomes the main challenge in practice. To tackle this issue, various Riemannian metrics have been proposed to guarantee the manifoldness, including Affine-Invariant Metric (AIM) (Pennec et al., 2006), Log-Euclidean Metric (LEM) (Arsigny et al., 2005), and Log-Cholesky Metric (LCM) (Lin, 2019), to name a

¹Dept. of Information Engineering and Computer Science, University of Trento, Trento, Italy ²School of Artificial Intelligence and Computer Science, Jiangnan University, Wuxi, China ³School of Electronics and Computer Science, University of Southampton, Southampton, U.K.. Correspondence to: Xiao-Jun Wu <wu_xiaojun@jiangnan.edu.cn>, Nicu Sebe <sebe@disi.unitn.it>.

few. Equipped with these metrics, many Euclidean methods could be generalized into the domain of the Riemannian manifold (Wang et al., 2012; Huang et al., 2015b;a; Harandi et al., 2018; Chen et al., 2021).

Recently, inspired by the vivid progress of deep learning (Hochreiter & Schmidhuber, 1997; Krizhevsky et al., 2012; He et al., 2016), following the theories of Riemannian geometry, several deep networks were designed on the SPD manifold. The principal motivation of these networks is to generalize the basic network components (transformation, activation, and classification) from Euclidean networks into Riemannian ones. For instance, Huang & Van Gool (2017) propose a densely connected feedforward network on the SPD manifold that is named SPDNet, successfully preserving SPDness in each layer. To generalize the object to SPD tensors, Chakraborty et al. (2020); Zhang et al. (2020) establish Riemannian convolutional networks correspondingly. In terms of distribution control, Brooks et al. (2019a) and Chakraborty (2020) alternately extend the normalization onto manifolds. In Nguyen (2021), based on a novel Gaussian embedding, an SPD deep network is proposed with the ability to mine the statistics in SPD deep features. For sequential SPD-valued data, a statistical recurrent unit (SPD-SRU) (Chakraborty et al., 2018), a dilated convolutional network (Zhen et al., 2019), and an RNN (Nguyen, 2022) based on Gyrovector space have been proposed. In the meantime, some works attempt to aggregate Riemannian approaches into traditional deep learning. For example, in Wang et al. (2020); Gao et al. (2021); Song et al. (2021), a square root layer is proposed to approximate Euclidean projection to alleviate the computational complexity manifesting in covariance pooling. Song et al. (2022) further propose a differentiable implementation for fast computation of the widely used square root and inverse square root.

In general, Riemannian methods, including deep or shallow methods, heavily rely on the Riemannian operators like geodesic, exponential & logarithmic maps, and parallel transportation. These operators are all induced from Riemannian metrics, which is a fundamental issue for machine learning. However, the existing Riemannian metrics on SPD manifolds fail to be learnable and hence cannot adapt to SPD-valued data. This flaw might undermine the effectiveness of Riemannian algorithms, especially for Rie-

mannian deep learning. To mitigate this limitation, in this paper we first re-analyze two popular Riemannian metrics on SPD manifolds and propose a general framework for designing Riemannian metrics by exploring the pullback technique (Tu, 2011). Following this guideline, we propose adaptive Riemannian metrics on SPD manifolds, which can be applied to any Riemannian methods on SPD manifolds. As such, our **contributions** are summarized as follows: **(a)** We uncover the essence of two popular Riemannian metrics and propose a general framework for designing Riemannian metrics; **(b)** Based on our framework, we propose specific adaptive Riemannian metrics on SPD manifolds and conduct comprehensive analyses in terms of the algebraic, analytic, and geometric properties; **(c)** Extensive experiments on widely used SPD learning benchmarks demonstrate that our metric exhibits consistent performance gain.

2. Basic Notations and Preliminaries

Some background about differential manifolds (Tu, 2011; Lee, 2013), and LEM (Arsigny et al., 2005) & LCM (Lin, 2019) on the SPD manifold are required in this paper. Due to the page limit, the typical basic notation is introduced here. A more detailed review is referred to Appendix A.

We denote the set of $n \times n$ SPD matrices as \mathcal{S}_{++}^n , the set of $n \times n$ symmetric matrices as \mathcal{S}^n , all the Cholesky matrices as \mathcal{L}_+^n , and all the $n \times n$ lower triangular matrices as \mathcal{L}^n . As shown in the previous literature (Arsigny et al., 2005; Lin, 2019), \mathcal{S}_{++}^n and \mathcal{L}_+^n form an SPD manifold and a Cholesky manifold, respectively. For an SPD matrix S , the matrix logarithm $\phi_{mln}(\cdot) : \mathcal{S}_{++}^n \rightarrow \mathcal{S}^n$ is defined as

$$\phi_{mln}(S) = U \ln(\Sigma) U^\top, \quad (1)$$

where $S = U \Sigma U^\top$ is the eigendecomposition, and $\ln(\cdot)$ is the diagonal natural logarithm. we define the Cholesky logarithm $\phi_{cln}(\cdot) : \mathcal{S}_{++}^n \rightarrow \mathcal{L}^n$ as

$$\phi_{cln}(S) = \varphi_{ln}(\mathcal{L}(S)) \quad (2)$$

where $L = \mathcal{L}(S)$ is the Cholesky decomposition ($S = LL^\top$), $\varphi_{ln}(L) = [L] + \ln(\mathbb{D}(L))$ is a coordinate system from the manifold \mathcal{L}_+^n onto the Euclidean space \mathcal{L}^n (Lin, 2019), $[L]$ is the strictly lower triangular part of L , $\mathbb{D}(L)$ is the diagonal entries. In Arsigny et al. (2005), LEM and vector space on \mathcal{S}_{++}^n are induced by matrix logarithm. In Lin (2019), LCM and Lie group on \mathcal{S}_{++}^n are derived from \mathcal{L}_+^n .

Definition 2.1 (Pullback Metrics). Suppose \mathcal{M}, \mathcal{N} are smooth manifolds, g is a Riemannian metric on \mathcal{N} , and $f : \mathcal{M} \rightarrow \mathcal{N}$ is smooth. Then the pullback of the tensor field g by f is defined point-wisely,

$$(f^* g)_p(V_1, V_2) = g_{f(p)}(f_{*,p}(V_1), f_{*,p}(V_2)), \quad (3)$$

where $p \in \mathcal{M}$, $f_{*,p}(\cdot)$ is the differential map of f at p , and $V_i \in T_p \mathcal{M}$. If $f^* g$ is positive definite, it is a Riemannian

metric on \mathcal{M} , which is called the pullback metric defined by f .

In the following, we will rely on pullback metrics to rethink LEM and LCM, and further unveil their common mathematical logic, which delivers direct formulation to our design of Riemannian metrics.

3. Rethinking LEM and LCM

Among the existing Riemannian metrics on the SPD manifold, LEM is popular in many applications given its closed form for the Fréchet mean and clear vector space & Lie group structures. In addition, the nascent LCM also shares similar properties with LEM and is gaining increasing attention. LEM is derived from the Lie group translation (Arsigny et al., 2005), while LCM is derived by the Cholesky decomposition, *i.e.* a Riemannian isometry from \mathcal{S}_{++}^n into \mathcal{L}_+^n (Lin, 2019). At first glance, one might think that LEM and LCM are designed by different mathematical tools. However, theoretically, the mathematical logic beneath their derivation can be the same. Specifically, both of them are pullback metrics from the Euclidean space. Denote LEM, LCM, and Euclidean metric as g^{LE} , g^{LC} and g^{E} , respectively. We have the following theorem.

Theorem 3.1. *On \mathcal{S}_{++}^n , $g^{\text{LE}} = \phi_{mln}^* g^{\text{E}}$ and $g^{\text{LC}} = \phi_{cln}^* g^{\text{E}}$. In other words, g^{LE} is a pullback metric from g^{E} by ϕ_{mln} , with ϕ_{mln} as a Riemannian isometry from $\{\mathcal{S}_{++}^n, g^{\text{LE}}\}$ to $\{\mathbb{R}^{n(n+1)/2}, g^{\text{E}}\}$. So does g^{LC} with ϕ_{cln} .*

Theorem 3.1 indicates that, as a Riemannian isometry, matrix logarithm (Cholesky logarithm) induces a Riemannian metric on \mathcal{S}_{++}^n from the Euclidean space $\mathbb{R}^{n(n+1)/2}$.

4. Adaptive Riemannian Metrics

Theorem 3.1 offers excellent examples of designing Riemannian metrics by pullback operations. Also, other properties like Lie groups and linear spaces are also related to ϕ_{mlog} or ϕ_{clog} on SPD manifolds. In this section, we will formulate and generalize this essence, forming our adaptive Riemannian metrics. Instead of presenting our results in an ad-hoc manner, we first present a general framework on how to build Riemannian metrics on arbitrary manifolds by the idea of pullback, together with analysis of associated algebraic and analytic properties. Then we proceed to focus on the specific case of the SPD manifold and introduce our adaptive Riemannian metrics.

4.1. General Framework

In Section 3, we have shown how LEM is derived from matrix logarithm ϕ_{mlog} . Besides, as shown in Arsigny et al. (2005), operations in Lie group and linear space on \mathcal{S}_{++}^n are also induced from ϕ_{mlog} . Now let us explain further

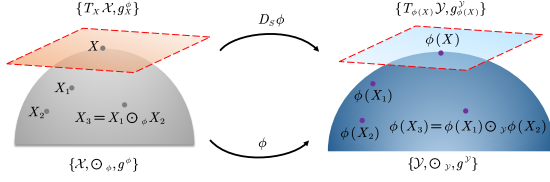


Figure 1. Conceptual illustration of Lemma 4.1. ϕ is a diffeomorphism from the smooth manifold \mathcal{X} to the Riemannian manifold $\{\mathcal{Y}, g^{\mathcal{Y}}\}$ with the Lie group multiplication $\odot_{\mathcal{Y}}$. With element multiplication \odot_{ϕ} defined in the co-domain of ϕ , $\{\mathcal{X}, \odot_{\phi}\}$ forms a Lie group. Endowed with the pullback metric $g^{\phi} = \phi^* g^{\mathcal{Y}}$, $\{\mathcal{X}, g^{\phi}\}$ forms a Riemannian manifold.

the underlying mechanism. $\phi_{mlog} : \mathcal{S}_{++}^n \rightarrow \mathcal{S}^n$ is an isomorphism in the category of smooth manifold (Tu, 2011), a diffeomorphism (a smooth bijection with a smooth inverse). The property of bijection offers the possibility of transferring algebraic and analytic structures from \mathcal{S}^n into \mathcal{S}_{++}^n . The smoothness of ϕ_{mlog} and its inverse suggest that smooth structures can be transferred into \mathcal{S}_{++}^n , like the Lie group and metric. More generally, given an arbitrary isomorphism $\phi : \mathcal{X} \rightarrow \mathcal{Y}$, it suffices to induce various properties from \mathcal{Y} into \mathcal{X} by ϕ as well.

Lemma 4.1. *Supposing $\phi : \mathcal{X} \rightarrow \mathcal{Y}$ is a bijection with its inverse map denoted as ϕ^{-1} , we have the following conclusion.*

1. *If \mathcal{Y} is a Hilbert space over the number field \mathbb{K} , \mathcal{X} forms a Hilbert space over \mathbb{K} , with the induced operations*

$$x_1 \odot_{\phi} x_2 = \phi^{-1}(\phi(x_1) \odot_{\mathcal{Y}} \phi(x_2)), \quad (4)$$

$$k \circledast_{\phi} x_2 = \phi^{-1}(k \circledast_{\mathcal{Y}} \phi(x_2)), \quad (5)$$

$$\langle x_1, x_2 \rangle_{\phi} = \langle \phi(x_1), \phi(x_2) \rangle_{\mathcal{Y}}, \quad (6)$$

where $x_1, x_2 \in \mathcal{X}$, $k \in \mathbb{K}$, and $\odot_{\mathcal{Y}}$, $\circledast_{\mathcal{Y}}$, $\langle \cdot, \cdot \rangle_{\mathcal{Y}}$ denote the element-wise multiplication, scalar multiplication, inner product in \mathcal{Y} , respectively. Besides, ϕ is a linear isomorphism preserving the inner product.

2. *If ϕ is a diffeomorphism between smooth manifold \mathcal{X} and (abelian) Lie group $\{\mathcal{Y}, \odot_{\mathcal{Y}}\}$, then $\{\mathcal{X}, \odot_{\phi}\}$ forms a (an) (abelian) Lie group, and ϕ is a Lie group isomorphism.*
3. *If ϕ is a diffeomorphism between smooth manifold \mathcal{X} and Riemannian manifold $\{\mathcal{Y}, g^{\mathcal{Y}}\}$, then the pullback metric $g^{\phi} = \phi^* g^{\mathcal{Y}}$ makes $\{\mathcal{X}, g^{\phi}\}$ an isometric Riemannian manifold to $\{\mathcal{Y}, g^{\mathcal{Y}}\}$ and ϕ is a Riemannian isometry.*

Lemma 4.1 indicates that a bijection can be an isomorphism, as long as it conforms with the axioms in a specific category.

In this way, various structural properties can be transferred from \mathcal{Y} to \mathcal{X} . Therefore, the key idea of this theorem lies in the proper map ϕ . For a better understanding, a conceptual illustration of case 2 and case 3 in Lemma 4.1 is shown in Figure 1.

In case 3 of Lemma 4.1, since ϕ is a Riemannian isometry, Riemannian operations like exponential & logarithmic maps and parallel transportation in \mathcal{X} can be induced from \mathcal{Y} as well. Note that on manifolds, the exponential & logarithmic maps do not generally exist globally (Do Carmo & Flaherty Francis, 1992). However, on SPD manifolds, there are global exponential & logarithmic maps. Following Lemma 4.1, we present general results on SPD manifolds. Notice that the only difference between Lemma 4.1 and the following one is that some Riemannian operators exist globally.

Theorem 4.2. *Let $S_1, S_2 \in \mathcal{S}_{++}^n$, $k \in \mathbb{R}$ and g^E be the standard Euclidean metric tensor field in $\mathbb{R}^{n(n+1)/2}$. $\phi : \mathcal{S}_{++}^n \rightarrow \mathcal{S}^n$ is a diffeomorphism. We define the following operations,*

$$S_1 \odot_{\phi} S_2 = \phi^{-1}(\phi(S_1) + \phi(S_2)), \quad (7)$$

$$k \circledast_{\phi} S_2 = \phi^{-1}(k\phi(S_2)), \quad (8)$$

$$\langle S_1, S_2 \rangle_{\phi} = g_I^E(\phi(S_1), \phi(S_2)), \quad (9)$$

$$g^{\phi} = \phi^* g^E. \quad (10)$$

Then, we have the following conclusions:

1. $\{\mathcal{S}_{++}^n, \odot_{\phi}, \circledast_{\phi}, \langle \cdot, \cdot \rangle_{\phi}\}$ is a Hilbert space over \mathbb{R} .
2. $\{\mathcal{S}_{++}^n, \odot_{\phi}\}$ is an abelian Lie group. $\{\mathcal{S}_{++}^n, g^{\phi}\}$ is a Riemannian manifold. g^{ϕ} is a bi-invariant metric. The associated geodesic distance is

$$d^{\phi}(S_1, S_2) = \|\phi(S_1) - \phi(S_2)\|_F. \quad (11)$$

The Riemannian operators are as follows

$$\text{Exp}_{S_1} V = \phi^{-1}(\phi(S_1) + \phi_{*,S_1} V), \quad (12)$$

$$\text{Log}_{S_1} S_2 = \phi_{*,\phi(S_1)}^{-1}(\phi(S_2) - \phi(S_1)), \quad (13)$$

$$\Gamma_{S_1 \rightarrow S_2}(V) = \phi_{*,\phi(S_2)}^{-1} \circ \phi_{*,S_1}(V), \quad (14)$$

where $V \in T_{S_1} \mathcal{S}_{++}^n$ is a tangent vector, Exp, Log and Γ are Riemannian exponential map, logarithmic map and parallel transportation respectively, and ϕ_* & ϕ_{*}^{-1} are the differential maps of ϕ & ϕ^{-1} .

3. ϕ is an isomorphism: (a) a linear isomorphism preserving the inner product; (b) a Lie group isomorphism; (3) a Riemannian isometry.

Remark 4.3. For a better understanding of the above theorem, we make the following remarks:

1. For the Hilbert space in case 1, the distance induced by the inner product $\langle \cdot, \cdot \rangle_\phi$ respects the geometry of SPD manifolds, as it is exactly the geodesic distance induced from g^ϕ .
2. For Eq. 14, as $(\phi^{-1})_* = (\phi_*)^{-1}$ (Tu, 2011), we simply write ϕ_*^{-1} . Besides, although $\phi_*^{-1}\phi_* = \mathbb{1}$ at any point, for $S_i \in \mathcal{S}_{++}^n$, $\phi_{*,\phi(S_2)}^{-1}\phi_{*,S_1}$ might not be the identity map. Specifically, $\phi_{*,\phi(S)}^{-1}\phi_{*,S} = \mathbb{1}_{T_S\mathcal{S}_{++}^n}$ does not imply $\phi_{*,\phi(S_2)}^{-1}\phi_{*,S_1} = \mathbb{1}_{T_{S_1}\mathcal{S}_{++}^n}$. In addition, $\phi_{*,S_2}^{-1}\phi_{*,S_1}$ could vary for different pairs of S_1, S_2 . In other words, the formulae of parallel transportation could be different among different pairs of S_1, S_2 .

In fact, LEM and LCM are special cases of Theorem 4.2, as ϕ_{mln} and ϕ_{cln} are instantiations of ϕ , and so do linear space & Lie group in Arsigny et al. (2005) and Lie group in Lin (2019). In addition, neither Arsigny et al. (2005) nor Lin (2019) reveals the Hilbert space structures in \mathcal{S}_{++}^n .

4.2. Adaptive Riemannian Metrics on SPD Manifolds

The key of Theorem 4.2 lies in ϕ . As long as we have a proper ϕ , Riemannian metrics on SPD manifolds can be induced. In the following, we will present our mappings and then discuss the induced metrics.

As an eigenvalues function, matrix logarithm in Eq. 1 is reduced into a scalar logarithm, which is a diffeomorphism between \mathbb{R}_+ and \mathbb{R} . Following this hint, the eigenvalues-based diffeomorphisms between \mathcal{S}_{++}^n and \mathcal{S}^n are reduced to scalar diffeomorphisms between \mathbb{R}_+ and \mathbb{R} . A very natural idea is to substitute the natural logarithm by scalar logarithms with an arbitrary proper base. In particular, we first define a general diagonal logarithm $\log(\cdot)$ as

$$\log_\alpha(X) = \text{diag}(\log_{a_1}^{x_{11}}, \log_{a_2}^{x_{22}}, \dots, \log_{a_n}^{x_{nn}}), \quad (15)$$

where $\alpha = (a_1, a_2, \dots, a_n) \in \mathbb{R}_+^n \setminus \{(1, 1, \dots, 1)\}$ is the base vector, diag is the diagonalization operator, and X is an $n \times n$ diagonal matrix. By abuse of notation, we denote $\log_\alpha(\cdot)$ as $\log(\cdot)$ for a general diagonal logarithm, and $\log_a^{(\cdot)}$ as $\log^{(\cdot)}$ for a general scalar logarithm. Specially, $a_1 = a_2 = \dots = a_n = e \Rightarrow \log(\cdot) = \ln(\cdot)$. Together with eigendecomposition, a general matrix logarithm could be derived:

$$\phi_{mlog}(S) = U \log_\alpha(\Sigma) U^\top, \quad (16)$$

where $S = U \Sigma U^\top$ is the eigendecomposition. As a special case, when $\alpha = (e, e, \dots, e)$, $\phi_{mlog} = \phi_{mln}$. Similar to the scalar logarithm, we have the following proposition.

Proposition 4.4 (Diffeomorphism). ϕ_{mlog} is a diffeomorphism, a smooth bijection with a smooth inverse $\phi_{mlog}^{-1}(\cdot) : \mathcal{S}^n \rightarrow \mathcal{S}_{++}^n$ defined as

$$\phi_{mlog}^{-1}(X) = \phi_{ma}(X) = U \alpha(\Sigma) U^\top, \quad (17)$$

where $\alpha(\Sigma) = \text{diag}(a_1^{\Sigma_{11}}, a_2^{\Sigma_{22}}, \dots, a_n^{\Sigma_{nn}})$ is a diagonal exponentiation.

Remark 4.5. Note that, ϕ_{mlog} should be more precisely understood as an arbitrary one from the following family

$$\{\phi_{mlog}^\alpha | \alpha = (a_1, \dots, a_n) \in \mathbb{R}_+^n \setminus \{(1, \dots, 1)\}\}. \quad (18)$$

By abuse of notation, we will simply use ϕ_{mlog} .

Since ϕ_{mlog} is a diffeomorphism from \mathcal{S}_{++}^n onto $\mathcal{S}^n \simeq \mathbb{R}^{n(n+1)/2}$, all the results in Theorem 4.2 holds.

Corollary 4.6. Following the notations in Theorem 4.2, we define \odot_{mlog} , \circledast_{mlog} , and $\langle \cdot, \cdot \rangle_{mlog}$, and g^{mlog} as Eq. 7-Eq. 10. Then, we have the following conclusions:

1. $\{\mathcal{S}_{++}^n, \odot_{mlog}, \circledast_{mlog}, \langle \cdot, \cdot \rangle_{mlog}\}$ is a Hilbert space over \mathbb{R} .
2. $\{\mathcal{S}_{++}^n, \odot_{mlog}\}$ is an abelian Lie group. g^{mlog} is a Riemannian metric over \mathcal{S}_{++}^n . We name this metric as Adaptive Log-Euclidean Metric (ALEM) and denote g^{mlog} as g^{ALE} . The geodesic distance under ALEM is

$$d^{\text{ALE}}(S_1, S_2) = \|\phi_{mlog}(S_1) - \phi_{mlog}(S_2)\|_{\text{F}}. \quad (19)$$

The associated Riemannian operators are as follows

$$\text{Exp}_{S_1} V = \phi_{ma}(\phi_{mlog}(S_1) + \phi_{mlog*,S_1} V), \quad (20)$$

$$\text{Log}_{S_1} S_2 = \phi_{ma*,X_1}(\phi_{mlog}(S_2) - \phi_{mlog}(S_1)), \quad (21)$$

$$\Gamma_{S_1 \rightarrow S_2}(V) = \phi_{ma*,X_2} \circ \phi_{mlog*,S_1}(V), \quad (22)$$

where $X_i = \phi_{mlog}(S_i) \in \mathcal{S}^n$.

3. ϕ_{mlog} is an isomorphism: (a) a linear isomorphism preserving the inner product; (b) a Lie group isomorphism; (3) a Riemannian isometry.

Remark 4.7. Obviously, ALEM would vary with different ϕ_{mlog} . This is why we use the plural to describe our metrics in the title. Besides, our metrics could be learnable. This is why we call them adaptive metrics.

Given the differential maps of ϕ_{mlog} and ϕ_{ma} , we can obtain the concrete formulae for Eq. 20-Eq. 22. We present their differential maps in the following.

Proposition 4.8 (Differentials). For a tangent vector $V \in T_S \mathcal{S}_{++}^n$, the differential $\phi_{mlog*,S} : T_S \mathcal{S}_{++}^n \rightarrow T_{\phi_{mlog}(S)} \mathcal{S}^n$ of ϕ_{mlog} at $S \in \mathcal{S}_{++}^n$ is given by

$$\phi_{mlog*,S}(V) = Q + Q^\top + W, \quad (23)$$

where $Q = D_U \log(\Sigma) U^\top$,

$$D_U = ((\sigma_1 I - S)^+ V u_1 \quad \dots \quad (\sigma_n I - S)^+ V u_n),$$

$$W = U \text{diag}\left(\frac{u_1^\top V u_1}{\sigma_1 \ln a_1}, \dots, \frac{u_n^\top V u_n}{\sigma_n \ln a_n}\right) U^\top,$$

$(\cdot)^+$ is the Moore–Penrose inverse, u_1, \dots, u_n are orthonormal eigenvectors of S , and the associated eigenvalues are $\sigma_1, \dots, \sigma_n$.

Symmetrically, for a tangent vector $\tilde{V} \in T_X \mathcal{S}^n$, the differential $\phi_{ma*,X} : T_X \mathcal{S}^n \rightarrow T_{\phi_{ma}(X)} \mathcal{S}_{++}^n$ of ϕ_{ma} at $X \in \mathcal{S}^n$ is given by

$$\phi_{ma*,X}(\tilde{V}) = \tilde{Q} + \tilde{Q}^\top + \tilde{W}, \quad (24)$$

where $S = \tilde{U} \tilde{\Sigma} \tilde{U}^\top$ is the eigendecomposition, $D_{\tilde{U}}$ is defined similarly, $\tilde{Q} = D_{\tilde{U}} \alpha(\tilde{\Sigma}) \tilde{U}^\top$, and

$$\tilde{W} = \tilde{U} \operatorname{diag}(\ln^{a_1} a_1^{\tilde{\sigma}_1} \tilde{u}_1^\top \tilde{V} \tilde{u}_1, \dots, \ln^{a_n} a_n^{\tilde{\sigma}_n} \tilde{u}_n^\top \tilde{V} \tilde{u}_n) \tilde{U}^\top.$$

In [Arsigny et al. \(2005\)](#), the differential of the matrix exponential is written as infinite series. The differential of our ϕ_{ma} can also be rewritten in this way.

Proposition 4.9 (Differential as Infinite Series). *Following the notation in Proposition 4.8, the differential of ϕ_{ma} can also be formulated as*

$$\begin{aligned} \phi_{ma*,X}(\tilde{V}) \\ = \sum_{k=1}^{\infty} \frac{1}{k!} \sum_{l=0}^{k-1} (\tilde{P}X)^{k-l-1} (D_{\tilde{P}}X + \tilde{P}\tilde{V})(\tilde{P}X)^l, \end{aligned} \quad (25)$$

where $\tilde{P} = \tilde{U}B\tilde{U}^\top$, $B = \operatorname{diag}(\ln^{a_1}, \dots, \ln^{a_n})$, $D_{\tilde{P}} = D_{\tilde{U}}B\tilde{U}^\top + \tilde{U}BD_{\tilde{U}}^\top$.

When ϕ_{ma} is reduced into matrix exponential, Eq. 25 becomes Eq. 8 in [Arsigny et al. \(2005\)](#), and our ALEM becomes exactly LEM. This is reasonable as our ϕ_{mlog} covers the matrix logarithm as a special case.

5. Properties of the Proposed Metrics

Since the involved diffeomorphism ϕ_{mlog} generalizes matrix logarithm, ALEM is indeed an adaptive generalization of LEM. Therefore, intuitively, ALEM would share every property of LEM. In this section, we will present some useful properties of our ALEM for machine learning, including Fréchet mean and invariance properties. All of the properties are shared by LEM, as LEM is a special case of our ALEM.

Fréchet means are important tools for SPD matrices learning ([Harandi et al., 2018; Chakraborty et al., 2018; Brooks et al., 2019a; Chakraborty, 2020](#)). Like LEM, our ALEM also enjoys closed forms of Fréchet means. We present a more general result, the weighted Fréchet mean, including the Fréchet mean as a special case. The following proposition indicates that the weighted Fréchet mean corresponds to the weighted mean in the logarithmic domain.

Proposition 5.1 (Weighted Fréchet Means). *For m points S_1, \dots, S_m in SPD manifolds with associated weights $w_1, \dots, w_m \in \mathbb{R}_+$, the weighted Fréchet mean M over the metric space $\{\mathcal{S}_{++}^n, d^{\text{ALE}}\}$ has a closed form*

$$M = \phi_{ma} \left(\sum_{i=1}^m \frac{w_i}{\sum_{j=1}^m w_i} \phi_{mlog}(S_i) \right). \quad (26)$$

Like LEM, although our ALEM does not conform with the affine-invariance, our ALEM enjoys some other kinds of invariance.

Proposition 5.2 (Bi-invariance). *ALEM is a Lie group bi-invariant metric.*

Proposition 5.3 (Exponential Invariance). *The Fréchet means under ALEM are exponential-invariant. In other words, for $S_1, \dots, S_m \in \mathcal{S}_{++}^n$ and $\beta \in \mathbb{R}$,*

$$(\operatorname{FM}(S_1, \dots, S_m))^\beta = \operatorname{FM}(S_1^\beta, \dots, S_m^\beta), \quad (27)$$

where $\operatorname{FM}(S_1, \dots, S_m)$ means the Fréchet mean of S_1, \dots, S_m .

Proposition 5.4 (Similarity Invariance). *The geodesic distance under ALEM is similarity invariant. In other words, let $R \in SO(n)$ be a rotation matrix, $s \in \mathbb{R}_+$ is a scale factor. Given any two SPD matrices S_1 and S_2 , we have*

$$d^{\text{ALE}}(S_1, S_2) = d^{\text{ALE}}(s^2 R S_1 R^\top, s^2 R S_2 R^\top). \quad (28)$$

Let us explain a bit more about the above three kinds of invariance. Firstly, among metrics on Lie groups, bi-invariant metrics are the most convenient ones ([Sternberg, 1999](#), Chapter V). Secondly, exponential-invariance offers a fast computation for Fréchet means under exponential scaling. At last, similarity-invariance is significant for describing the frequently encountered covariance matrices ([Arsigny et al., 2005](#)).

So far, the above discussion focuses on theoretical analysis. Now, let us reconsider Eq. 16 in a numerical way.

Proposition 5.5. ϕ_{mlog} can be rewritten as

$$\phi_{mlog}(S) = U \log_\alpha(\Sigma) U^\top, \quad (29)$$

$$= U A \ln(\Sigma) U^\top, \quad (30)$$

$$= U \frac{\ln(\Sigma)}{B} U^\top, \quad (31)$$

where $\frac{X}{Y}$ is the diagonal division, $B = \operatorname{diag}(\ln^{a_1}, \dots, \ln^{a_n})$, and $A = \frac{I}{B}$.

Based on the above proposition, more analyses could be carried out from a numerical point of view. First, $\phi_{mlog}(\cdot)$ can balance the eigenvalues of an input SPD matrix S by exploiting different bases for different eigenvalues. In Riemannian algorithms, manifold-valued features usually contain

vibrant information. We expect that by the above adaptation, manifold-valued data could be better fitted and the learning ability of algorithms could be further promoted.

Remark 5.6. Note that the design and analysis in Section 4.2 and Section 5 can be readily transferred into LCM, generating an adaptive version of LCM.

6. Applications to SPD Neural Networks

Since Riemannian metrics are foundations of Riemannian learning algorithms, our ALEM has the potential to rewrite Riemannian algorithms. Besides, the base vector in ϕ_{mlog} could bring vibrant diversity of our ALEM. This adaptive mechanism could help the algorithm better fit with complex manifold-valued data. Especially in Riemannian neural networks, as we will show, optimization of base vectors can be easily embedded into the standard backpropagation (BP) process. Therefore, we focus on the applications of our metrics to SPD neural networks.

In the existing SPD neural networks, on activation or classification layers, SPD features would interact with the logarithmic domain by matrix logarithm (Huang & Van Gool, 2017; Zhen et al., 2019; Chakraborty et al., 2020; Nguyen, 2021). The underlying mechanism of this interaction is that matrix logarithm is an isomorphism, identifying the Riemannian manifold $\{\mathcal{S}_{++}^n, g^{LE}\}$ with the Euclidean space \mathcal{S}^n . This projection can therefore maintain the LEM-based geometry of SPD features. However, in deep networks, the geometry might be more complex. Since ALEM can vibrantly adapt with network learning, compared with the plain LEM, our ALEM could more faithfully respect the geometry of SPD deep features. As an identification of $\{\mathcal{S}_{++}^n, g^{ALE}\}$ and \mathcal{S}^n , ϕ_{mlog} thus possesses more advantages than the fixed ϕ_{mln} . We therefore replace the vanilla matrix logarithm with our ϕ_{mlog} , to respect the more advantageous geometry, *i.e.* the ALEM-based geometry.

We focus on the most classic SPD network, SPDNet (Huang & Van Gool, 2017), where matrix logarithm is used for classification. Please refer to the Appendix A.4 for a quick review of SPDNet, if necessary. Specifically, matrix logarithm in the LogEig layer is substituted by our ϕ_{mlog} . We call this layer as adaptive logarithm (ALog) layer. We set the base vector α as a learnable parameter. In this way, as ϕ_{mlog} is an isomorphism, the network can implicitly respect the ALEM-based Riemannian metric by learning the ϕ_{mlog} explicitly. Besides, since our ALog layer is independent of specific network architectures, it can be plugged into other SPD deep networks as well.

7. Parameters Learning

Now let us explain how to optimize the proposed layer in a standard BP framework. The specificities of the proposed

ALog layer are the nonlinear manipulation of both inputs and parameters. In this section, we will first discuss the concrete way of updating the parameters and then move on to its gradient computation.

7.1. Parameters Update

Denote the dimension of an input SPD matrix S as $d \times d$. Rethinking Eq. 29-Eq. 31, we could observe that there are two ways of dealing with the parameters. The first approach, called *learning factors*, is to view the multiplier A or divisor B as parameters, which are both diagonal matrices. The second method, called *learning bases*, is to learn the base vector α directly, which lies in a non-Euclidean space $\mathbb{R}_+^d \setminus \{1, 1, \dots, 1\}$.

For the first way, since the parameters lie in a Euclidean space \mathbb{R}^d , the optimization can be easily integrated into the BP algorithm. We call learning A MUL and learning B DIV.

For the case of learning bases, since the parameter α lies in a non-Euclidean space, specific updating strategies should be considered. Note that the elements of α are pairwisely decoupled. Without loss of generality, we focus on the case of a scalar parameter $a > 0 \& a \neq 1$. The condition of $a \neq 1$ can be further waived since we can set $a = 1 + \epsilon$ if $a = 1$. Then there is only one constraint about positivity. To ensure this property is satisfied, we will learn it implicitly through an unconstrained parameter or explicitly through the Riemannian optimization (Absil et al., 2008). In detail, we can learn the shift-ReLU of an unconstrained parameter, *i.e.* $\max(\epsilon, a)$ with $\epsilon \in \mathbb{R}_+$. This strategy is named RELU. Other tricks like square are also feasible, but we will focus on the RELU. In addition, positive scalar a can be directly optimized by a geometric method, called GEOM. Specifically, we view a positive scalar as a point in a manifold, *i.e.* a 1-dimension SPD manifold. Then we have the following updating formula for GEOM.

Proposition 7.1. *Viewing a positive scalar a as a point in a 1-dimensional SPD manifold, we have the following updating formula for Riemannian stochastic gradient descent (RSGD).*

$$a^{(t+1)} = a^{(t)} e^{-\gamma^{(t)} a^{(t)} \nabla_{a^{(t)}} L}, \quad (32)$$

where $\nabla_{a^{(t)}} L$ is the Euclidean gradient of a at $a^{(t)}$, $\gamma^{(t)}$ is the learning rate, and $e^{(\cdot)}$ is the natural exponentiation.

Besides, by Eq. 32, we could prove that GEOM is equivalent to DIV, which is given in the following proposition.

Proposition 7.2. *For parameters learning in ϕ_{mlog} , optimizing the base vector α by RSGD is equivalent to optimizing divisor matrix B by Euclidean stochastic gradient descent (ESGD).*

Based on the above analysis, there are essentially three ways

of optimization, *i.e.*, RELU, DIV, and MUL.

7.2. Gradients Computation

There are two gradients that need calculation in the proposed ALog layer, one w.r.t the parameters and another w.r.t the input of the ALog layer. Since structural matrix decomposition is involved in ϕ_{mlog} , the following contents heavily rely on the structural matrix BP (Ionescu et al., 2015), the key idea of which is the invariance of first-order differential form. For the ALog layer, it is essentially a special case of eigenvalue functions. Based on the formula offered in Bhatia (2009) and matrix BP techniques presented in Ionescu et al. (2015); Song et al. (2021), we can obtain all the gradients, as presented in the following proposition.

Proposition 7.3. *Let us denote $X = \phi_{mlog}(S)$, where $S \in \mathcal{S}_{++}^d$ is an input SPD matrix of the ALog layer. We have the following gradients:*

$$\nabla_S L = U[K \odot (U^T(\nabla_X L)U)]U^T, \quad (33)$$

$$\nabla_A L = [U^T(\nabla_X L)U] \odot \log(\Sigma), \quad (34)$$

where $S = U\Sigma U^T$ is the eigendecomposition of an SPD matrix and matrix K is defined as

$$K_{ij} = \begin{cases} \frac{f(\sigma_i) - f(\sigma_j)}{\sigma_i - \sigma_j} & \text{if } \sigma_i \neq \sigma_j \\ f'(\sigma_i) & \text{otherwise} \end{cases} \quad (35)$$

where $f(\sigma_i) = A_{ii} \log_e(\sigma_i)$ and $\Sigma = \text{diag}(\sigma_1, \sigma_2, \dots, \sigma_d)$.

8. Experiments

In this section, we validate the efficacy of our approaches on multiple datasets. We would like to clarify that our method does not necessarily aim to achieve the SOTA in a general sense for the following tasks, but rather to promote the learning abilities of the family of SPD-based methods.

8.1. Datasets and Settings

As we discussed before, although the proposed ALog layers can be plugged into the existing SPD networks, we focus on the SPDNet framework (Huang & Van Gool, 2017). We follow the PyTorch code provided by SPDNetBN (Brooks et al., 2019a) to reproduce SPDNet & SPDNetBN and implement our approaches. We evaluate our methods on three datasets, the HDM05 (Müller et al., 2007) for skeleton-based actions recognition, the FPHA (Garcia-Hernando et al., 2018) for skeleton-based hand gestures recognition, and the AFEW (Dhall et al., 2018) for emotions recognition. The dimension of the input SPD features from the three datasets are 93×93 , 63×63 and 512×512 , respectively. For more details about the settings of the datasets, please refer to Appendix C.

Table 1. Results of ALog on the HDM05 dataset.

Architecture	{93, 30}	{93, 70, 30}	{93, 70, 50, 30}
γ	$1e^{-2}$		
SPDNet	62.92 \pm 0.81	62.87 \pm 0.60	63.03 \pm 0.67
SPDNetBN	63.03 \pm 0.75	58.27 \pm 1.7	52.02 \pm 2.34
ALog-MUL	63.52 \pm 0.75	63.86 \pm 0.58	63.94\pm0.44
ALog-DIV	63.60\pm0.79	63.93 \pm 0.52	63.81 \pm 0.7
ALog-RELU	63.02 \pm 0.79	63.94\pm0.64	63.14 \pm 0.65
γ	$5e^{-2}$		
SPDNet	63.89 \pm 0.73	64.00 \pm 0.65	63.72 \pm 0.61
SPDNetBN	63.75 \pm 0.69	48.78 \pm 5.15	37.84 \pm 6.10
ALog-MUL	64.4 \pm 0.68	64.60 \pm 0.69	64.36 \pm 0.49
ALog-DIV	64.81\pm0.64	64.84\pm0.65	64.80\pm0.36
ALog-RELU	63.97 \pm 0.75	64.10 \pm 0.63	63.78 \pm 0.46

We denote $\{d_0, d_1, \dots, d_L\}$ as the dimensions of each BiMap layer in SPDNet backbone. Following the settings in Brooks et al. (2019a), all networks are trained by the default SGD with a fixed learning rate γ , and with a batch size of 30. To make ALog start from the vanilla matrix logarithm, the parameters in MUL, DIV and RELU are initialized as 1, 1 and e , respectively. By abuse of notation, SPDNet-ALog-MUL is abbreviated as ALog-MUL, meaning we substitute the LogEig layer (matrix logarithm) in SPDNet with our proposed ALog optimized by MUL.

8.2. Experimental Results

On the three datasets, the training epochs are set to be 200, 500, and 100. We verify our ALog on the SPDNet with various architectures. Besides, we further test the robustness of the proposed layer against different learning rates on the HDM05 and FPHA datasets. Generally speaking, among all three kinds of optimization, MUL shows more robust performance gain and achieves consistent improvement over vanilla matrix logarithm. Besides, we could also observe that ALog-MUL is comparable to or even better than SPDNetBN, which yet brings much more complexity than our approach. The underlying reason is twofold. Firstly, the effectiveness of the Euclidean loss function applied to the Riemannian deep networks mainly depends on the Euclidean projection itself. Compared to the plain matrix logarithm, our ϕ_{mlog} not only incorporates matrix logarithm as a special case but also can adaptively respect the geometry of manifold-valued data. In addition, the implicitly induced algebraic and geometric structures discussed in Section 5 will be preserved by ϕ_{mlog} and could further promote the overall learning ability of the network. The following are detailed observations and analyses.

Results on the HDM05 dataset. The 10-fold results are presented in Table 1, where dataset split and weights initialization are randomized. On the HDM05 dataset, variations of the architectures come from the original paper of the

Table 2. Results of ALog on the FPHA dataset.

Methods	SPDNet	SPDNetBN	ALog-MUL	ALog-DIV	ALog-RELU
Acc.	85.73 \pm 0.80	86.83 \pm 0.74	87.8 \pm 0.71	88.07\pm1.13	86.65 \pm 0.68

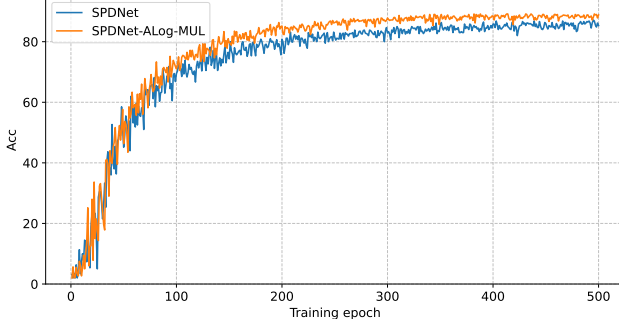


Figure 2. Accuracy curves on the FPHA dataset.

Table 3. Results of ALog on the AFEW dataset.

Number of BiMap Layers	1	2	3	4
SPDNet	48.53	46.89	48.24	47.22
SPDNetBN	46.89	46.65	47.62	48.35
ALog-MUL	48.57	48.13	49.45	50.62
ALog-DIV	48.42	48.02	48.13	49.89
ALog-RELU	48.06	47.25	48.86	48.1

SPDNet (Huang & Van Gool, 2017). Generally speaking, endowed with the ALog, SPDNet would achieve consistent improvement. Among all three kinds of optimization, RELU only brings limited improvement. The reason might be that RELU fails to respect the innate geometry of the positive constraint. There is another interesting observation worth mentioning. In Brooks et al. (2019a), only the result of SPDNetBN under the architecture of {93, 30} is reported on this dataset. Our experiments show that with the network going deeper, SPDNetBN tends to collapse, while our ALog layer performs robustly in all settings.

Results on the FPHA dataset. On this dataset, we validate our approach, with a learning rate of $1e^{-2}$, over 10-fold cross-validation on random initialization. Since our experiments show that the vanilla SPDNet is already saturated with 1 BiMap layer, we just report the results on the architecture of {63, 33}, which are presented in Table 2. We find that although DIV achieves the best performance on this dataset, it presents the biggest variance. The reason is that there is an underlying nonlinear scaling mechanism, which is discussed in Appendix D.1. However, ALog-MUL achieves robust improvement, and even surpasses SPDNetBN. This once again demonstrates the significance of our adaptive mechanism for Riemannian deep networks. Finally, in terms of convergence analysis, accuracy curves with and without ALog are reported in Figure 2 as well.

Results on the AFEW dataset. On this dataset, the learning rate is $5e^{-2}$ and we validate our method under four network architectures, *i.e.* {512,100}, {512,200,100}, {512,400,200,100}, and {512,400,300,200,100}. Note that, on this dataset, SPDNetBN tends to present relatively large fluctuations in performance, so we compute the median of the last ten epochs. On various architectures, consistent improvement can be observed when SPDNet is endowed with our ALog. In addition, MUL achieves the best among all three optimization tricks. Another interesting observation is that SPDNetBN seems not very effective on these deep features, while our methods show consistent superior performance, particularly obvious for our ALog-MUL. This indicates that our adaptive layer maintains effectiveness when applied to covariance matrices from deep features.

Model complexity. Our ALog manifests the same complexity no matter how it is optimized. Without loss of generality, the below discussion focuses on ALog-MUL. The extra computation and memory induced by the ALog layer are minor. It only depends on the final dimension of the network. Let us take the deepest one on the AFEW dataset as an example. Our ALog only brings 100 unconstrained scalar parameters, while SPDNetBN needs an SPD matrix parameter for each Riemannian batch normalization (RBN) layer. The total number of the parameters in RBN layers sums up to $400^2 + 300^2 + 200^2$, which is much more than ours. In addition, the SPDNetBN needs to store the running mean of SPD matrices in every RBN layer, while our ALog only needs to store a base vector. In terms of computation, the extra cost of our ALog is secondary as well. The forward and backward computation of our ALog is generally the same as the plain matrix logarithm, while computation in the RBN layer is much more complex. All in all, our ALog can consistently improve the performance of the SPDNet and achieve comparable or better results against SPDNetBN with much cheaper computation and memory costs.

9. Conclusion

Riemannian metrics are foundations for Riemannian learning algorithms. In this paper, we proposed a general framework for designing Riemannian metrics on arbitrary manifolds by pullback metrics. According to this framework, adaptive Riemannian metrics were introduced for SPD matrices learning. We also present comprehensive and rigorous theories of our metrics. Extensive experiments indicate that SPD deep networks can benefit from our metrics. Finally, we would like to point out some future avenues based on

this framework. The transformation and activation layers in SPD networks might be re-designed based on our metrics. Similar to Corollary 4.6, LCM can be also transferred into an adaptive version as well. Following the general framework in Lemma 4.1, it is also possible to design Riemannian metrics on other manifolds, like Grassmannian manifolds.

References

- Absil, P.-A., Mahony, R., and Sepulchre, R. *Optimization Algorithms on Matrix Manifolds*. Princeton University Press, 2008. URL <https://doi.org/10.1515/9781400830244>.
- Amari, S.-i. *Information geometry and its applications*, volume 194. Springer, 2016. URL <https://doi.org/10.1007/978-4-431-55978-8>.
- Arnaudon, M., Barbaresco, F., and Yang, L. Riemannian medians and means with applications to radar signal processing. *IEEE Journal of Selected Topics in Signal Processing*, 7(4):595–604, 2013. URL <https://doi.org/10.1109/JSTSP.2013.2261798>.
- Arsigny, V., Fillard, P., Pennec, X., and Ayache, N. *Fast and Simple Computations on Tensors with Log-Euclidean Metrics*. PhD thesis, INRIA, 2005. URL https://doi.org/10.1007/11566465_15.
- Bhatia, R. *Positive Definite Matrices*. Princeton University Press, 2009. URL <https://doi.org/10.1515/9781400827787>.
- Bonnabel, S. Stochastic gradient descent on Riemannian manifolds. *IEEE Transactions on Automatic Control*, 58(9):2217–2229, 2013. URL <https://arxiv.org/abs/1111.5280>.
- Brooks, D., Schwander, O., Barbaresco, F., Schneider, J.-Y., and Cord, M. Riemannian batch normalization for SPD neural networks. In *Advances in Neural Information Processing Systems*, volume 32, 2019a. URL <https://arxiv.org/abs/1909.02414>.
- Brooks, D. A., Schwander, O., Barbaresco, F., Schneider, J.-Y., and Cord, M. Exploring complex time-series representations for Riemannian machine learning of radar data. In *ICASSP 2019-2019 IEEE International Conference on Acoustics, Speech and Signal Processing (ICASSP)*, pp. 3672–3676. IEEE, 2019b. URL <https://doi.org/10.1109/ICASSP.2019.8683056>.
- Chakraborty, R. ManifoldNorm: Extending normalizations on Riemannian manifolds, 2020. URL <https://arxiv.org/abs/2003.13869>.
- Chakraborty, R., Yang, C.-H., Zhen, X., Banerjee, M., Archer, D., Vaillancourt, D., Singh, V., and Vemuri, B. A statistical recurrent model on the manifold of symmetric positive definite matrices. *Advances in Neural Information Processing Systems*, 31, 2018. URL <https://arxiv.org/abs/1805.11204>.
- Chakraborty, R., Bouza, J., Manton, J., and Vemuri, B. C. Manifoldnet: A deep neural network for manifold-valued data with applications. *IEEE Transactions on Pattern Analysis and Machine Intelligence*, 2020. URL <https://doi.org/10.1109/TPAMI.2020.3003846>.
- Chen, Z., Xu, T., Wu, X.-J., Wang, R., and Kittler, J. Hybrid Riemannian graph-embedding metric learning for image set classification. *IEEE Transactions on Big Data*, 2021. URL <https://doi.org/10.1109/TBDA.2021.3113084>.
- Dhall, A., Kaur, A., Goecke, R., and Gedeon, T. Emotiwi 2018: Audio-video, student engagement and group-level affect prediction. In *Proceedings of the 20th ACM International Conference on Multimodal Interaction*, pp. 653–656, 2018. URL <https://arxiv.org/abs/1808.07773>.
- Do Carmo, M. P. and Flaherty Francis, J. *Riemannian Geometry*, volume 6. Springer, 1992. URL <https://link.springer.com/book/9780817634902>.
- Gao, Z., Wang, Q., Zhang, B., Hu, Q., and Li, P. Temporal-attentive covariance pooling networks for video recognition. *Advances in Neural Information Processing Systems*, 34, 2021. URL <https://arxiv.org/abs/2110.14381>.
- Garcia-Hernando, G., Yuan, S., Baek, S., and Kim, T.-K. First-person hand action benchmark with RGB-D videos and 3D hand pose annotations. In *Proceedings of the IEEE Conference on Computer Vision and Pattern Recognition*, pp. 409–419, 2018. URL <https://arxiv.org/abs/1704.02463>.
- Guilleminot, J. and Soize, C. Generalized stochastic approach for constitutive equation in linear elasticity: a random matrix model. *International Journal for Numerical Methods in Engineering*, 90(5):613–635, 2012. URL <https://doi.org/10.1002/nme.3338>.
- Harandi, M., Salzmann, M., and Hartley, R. Dimensionality reduction on SPD manifolds: The emergence of geometry-aware methods. *IEEE Transactions on Pattern Analysis and Machine Intelligence*, 40(1):48–62, 2018. URL <https://doi.org/10.1109/TPAMI.2017.2655048>.

- He, K., Zhang, X., Ren, S., and Sun, J. Deep residual learning for image recognition. In *Proceedings of the IEEE Conference on Computer Vision and Pattern Recognition*, pp. 770–778, 2016. URL <https://arxiv.org/abs/1512.03385>.
- Hochreiter, S. and Schmidhuber, J. Long short-term memory. *Neural Computation*, 9(8):1735–1780, 1997. URL <https://doi.org/10.1162/neco.1997.9.8.1735>.
- Hua, X., Cheng, Y., Wang, H., Qin, Y., Li, Y., and Zhang, W. Matrix CFAR detectors based on symmetrized Kullback–Leibler and total Kullback–Leibler divergences. *Digital Signal Processing*, 69:106–116, 2017. URL <https://doi.org/10.1016/j.dsp.2017.06.019>.
- Huang, Z. and Van Gool, L. A Riemannian network for SPD matrix learning. In *Thirty-first AAAI conference on artificial intelligence*, 2017. URL <https://arxiv.org/abs/1608.04233>.
- Huang, Z., Wang, R., Shan, S., and Chen, X. Face recognition on large-scale video in the wild with hybrid euclidean-and-riemannian metric learning. *Pattern Recognition*, 48(10):3113–3124, 2015a. URL <https://doi.org/10.1016/j.patcog.2015.03.011>.
- Huang, Z., Wang, R., Shan, S., Li, X., and Chen, X. Log-Euclidean metric learning on symmetric positive definite manifold with application to image set classification. In *International Conference on Machine Learning*, pp. 720–729. PMLR, 2015b. URL <https://dl.acm.org/doi/abs/10.5555/3045118.3045196>.
- Ionescu, C., Vantzos, O., and Sminchisescu, C. Matrix backpropagation for deep networks with structured layers. In *Proceedings of the IEEE International Conference on Computer Vision*, pp. 2965–2973, 2015. URL <https://arxiv.org/abs/1509.07838>.
- Krizhevsky, A., Sutskever, I., and Hinton, G. E. Imagenet classification with deep convolutional neural networks. *Advances in Neural Information Processing Systems*, 25, 2012. URL <https://doi.org/10.1145/3065386>.
- Lee, J. M. *Introduction to Smooth Manifolds*. Springer, 2013. URL <https://doi.org/10.1007/978-1-4419-9982-5>.
- Lin, Z. Riemannian geometry of symmetric positive definite matrices via Cholesky decomposition. *SIAM Journal on Matrix Analysis and Applications*, 40(4):1353–1370, 2019. URL <https://arxiv.org/abs/1908.09326>.
- Magnus, J. R. and Neudecker, H. *Matrix differential calculus with applications in statistics and econometrics*. John Wiley & Sons, 2019. URL <https://doi.org/10.1002/9781119541219>.
- Meng, D., Peng, X., Wang, K., and Qiao, Y. Frame attention networks for facial expression recognition in videos. In *2019 IEEE International Conference on Image Processing (ICIP)*, pp. 3866–3870. IEEE, 2019. URL <https://arxiv.org/abs/1907.00193>.
- Moakher, M. On the averaging of symmetric positive-definite tensors. *Journal of Elasticity*, 82(3):273–296, 2006. URL <https://doi.org/10.1007/s10659-005-9035-z>.
- Müller, M., Röder, T., Clausen, M., Eberhardt, B., Krüger, B., and Weber, A. Documentation mocap database HDM05. Technical report, Universität Bonn, 2007. URL <https://resources.mpi-inf.mpg.de/HDM05/>.
- Nguyen, X. S. Geomnet: A neural network based on Riemannian geometries of SPD matrix space and Cholesky space for 3D skeleton-based interaction recognition. In *Proceedings of the IEEE International Conference on Computer Vision*, pp. 13379–13389, 2021. URL <https://arxiv.org/abs/2111.13089>.
- Nguyen, X. S. A Gyrovector space approach for symmetric positive semi-definite matrix learning. In *Proceedings of the European Conference on Computer Vision*, pp. 52–68, 2022. URL https://doi.org/10.1007/978-3-031-19812-0_4.
- Pennec, X., Fillard, P., and Ayache, N. A Riemannian framework for tensor computing. *International Journal of Computer Vision*, 66(1):41–66, 2006. URL <https://doi.org/10.1007/s11263-005-3222-z>.
- Song, Y., Sebe, N., and Wang, W. Why approximate matrix square root outperforms accurate SVD in global covariance pooling? In *Proceedings of the IEEE International Conference on Computer Vision*, pp. 1115–1123, 2021. URL <https://arxiv.org/abs/2105.02498>.
- Song, Y., Sebe, N., and Wang, W. Fast differentiable matrix square root and inverse square root. *arXiv preprint arXiv:2201.12543*, 2022. URL <https://arxiv.org/abs/2201.12543>.
- Sternberg, S. *Lectures on differential geometry*, volume 316. American Mathematical Soc., 1999. URL <https://www.ams.org/journals/bull/1965-71-02/S0002-9904-1965-11286-1/S0002-9904-1965-11286-1.pdf>.

Tu, L. W. *An Introduction to Manifolds*. Springer, 2011. URL https://doi.org/10.1007/978-1-4419-7400-6_3.

Wang, Q., Xie, J., Zuo, W., Zhang, L., and Li, P. Deep CNNs meet global covariance pooling: Better representation and generalization. *IEEE Transactions on Pattern Analysis and Machine Intelligence*, 43(8):2582–2597, 2020. URL <https://arxiv.org/abs/1904.06836>.

Wang, R., Guo, H., Davis, L. S., and Dai, Q. Covariance discriminative learning: A natural and efficient approach to image set classification. In *Proceedings of the IEEE Conference on Computer Vision and Pattern Recognition*, pp. 2496–2503. IEEE, 2012. URL <https://doi.org/10.1109/CVPR.2012.6247965>.

Yger, F. A review of kernels on covariance matrices for BCI applications. In *2013 IEEE International Workshop on Machine Learning for Signal Processing (MLSP)*, pp. 1–6. IEEE, 2013. URL <https://doi.org/10.1109/MLSP.2013.6661972>.

Zhang, T., Zheng, W., Cui, Z., Zong, Y., Li, C., Zhou, X., and Yang, J. Deep manifold-to-manifold transforming network for skeleton-based action recognition. *IEEE Transactions on Multimedia*, 22(11):2926–2937, 2020. URL <https://arxiv.org/abs/1705.10732>.

Zhen, X., Chakraborty, R., Vogt, N., Bendlin, B. B., and Singh, V. Dilated convolutional neural networks for sequential manifold-valued data. In *Proceedings of the IEEE International Conference on Computer Vision*, pp. 10621–10631, 2019. URL <https://arxiv.org/abs/1910.02206>.

A. Preliminaries

A.1. Smooth Manifolds

We first recap some basic definitions related to this work on smooth manifolds. For in-depth understanding, please kindly refer to [Tu \(2011\)](#); [Lee \(2013\)](#).

The most important properties of manifolds are locally Euclidean, which are described by coordinate systems.

Definition A.1 (Coordinate Systems, Charts, Parameterizations). A topological space \mathcal{M} is locally Euclidean of dimension n if every point in \mathcal{M} has a neighborhood U such that there is a homeomorphism ϕ from U onto an open subset of \mathbb{R}^n . We call the pair $\{U, \phi : U \rightarrow \mathbb{R}^n\}$ as a chart, U as a coordinate neighborhood, the homeomorphism ϕ as a coordinate map or coordinate system on U , and ϕ^{-1} as a parameterization of U .

Intuitively, a coordinate system is a bijection that locally identifies the Euclidean space with the manifold. It locally preserves the most basic properties in a manifold, the topology. Now, topological manifolds, which are foundations of smooth manifolds, can be defined.

Definition A.2 (Topological Manifolds). A topological manifold is a locally Euclidean, second countable, and Hausdorff topological space.

In smooth manifolds, compatibility is further required to define smooth structures or operations.

Definition A.3 (C^∞ -compatible). Two charts $\{U, \phi_1 : U \rightarrow \mathbb{R}^n\}, \{V, \phi_2 : V \rightarrow \mathbb{R}^n\}$ of a locally Euclidean space are C^∞ -compatible if the following two composite maps

$$\begin{aligned} \phi_1 \circ \phi_2^{-1} : \phi_2(U \cap V) \rightarrow \phi_1(U \cap V), \\ \phi_2 \circ \phi_1^{-1} : \phi_1(U \cap V) \rightarrow \phi_2(U \cap V) \end{aligned} \quad (36)$$

are C^∞ .

By abuse of notation, we view ϕ alternatively as a chart or map according to the context, and abbreviate C^∞ -compatible as compatible.

Definition A.4 (Atlases). A C^∞ atlas or simply an atlas on a locally Euclidean space \mathcal{M} is a collection $\mathcal{A} = \{\{U_\alpha, \phi_\alpha\}\}$ of pairwise C^∞ -compatible charts that cover \mathcal{M} .

An atlas \mathcal{A} on a locally Euclidean space is said to be maximal if it is not contained in a larger atlas. With a maximal atlas, smooth manifold can be defined.

Definition A.5 (Smooth Manifolds). A smooth manifold is defined as a topological manifold endowed with a maximal atlas.

We call the maximal atlas of a smooth manifold its differential structure. In addition, every atlas \mathcal{A} is contained in a unique maximal atlas \mathcal{A}^+ ([Tu, 2011](#)). Therefore, an atlas can be used to identify the differential structure of a smooth manifold. In this paper, manifolds always mean smooth manifolds. Now, we can define the smoothness of a map between manifolds.

Definition A.6 (Smoothness). Let \mathcal{N} and \mathcal{M} be smooth manifolds, and $f : \mathcal{N} \rightarrow \mathcal{M}$ a continuous map, $f(\cdot)$ is said to be C^∞ or smooth, if there are atlases \mathcal{A}_n for \mathcal{N} and \mathcal{A}_m for \mathcal{M} such that for every chart $\{U, \phi\}$ in \mathcal{A}_n and $\{V, \psi\}$ in \mathcal{A}_m , the map

$$\psi \circ F \circ \phi^{-1} : \phi(U \cap f^{-1}(V)) \rightarrow \mathbb{R}^m \quad (37)$$

is C^∞ .

In elementary calculus, smooth functions have derivatives. In manifolds, derivatives are generalized into differential maps.

Definition A.7 (Differential Maps). Let $f : \mathcal{N} \rightarrow \mathcal{M}$ be a C^∞ map between two manifolds. At each point $p \in \mathcal{N}$, the map f induces a linear map of tangent spaces, called its differential at p ,

$$f_{*,p} : T_p \mathcal{N} \rightarrow T_{f(p)} \mathcal{M}. \quad (38)$$

$f_{*,p}$ can be locally represented by the Jacobian matrix under a chart $\{U, \phi\}$ about p and a chart $\{V, \psi\}$ about $f(p)$,

$$f_{*,p} := \frac{\partial f}{\partial x} := \frac{\partial \psi f \phi^{-1}}{\partial x}, \quad (39)$$

where $\frac{\partial f}{\partial x}$ is called the derivative (Jacobian matrix) of f under the charts of $\{U, \phi\}$ and $\{V, \psi\}$.

With the definition of smoothness, it is possible to define smooth algebraic structures on a manifold, *i.e.* Lie groups. Intuitively, a Lie group is an integration of algebra (group) and geometry (manifold).

Definition A.8 (Lie Groups). A manifold is a Lie group, if it forms a group with a group operation \odot such that $m(x, y) \mapsto x \odot y$ and $i(x) \mapsto x^{-1}$ are both smooth, where x^{-1} is the group inverse of x .

A.2. Riemannian Manifolds

When manifolds are endowed with Riemannian metrics, various Euclidean operators can find their counterparts in manifolds. A plethora of discussions can be found in [Do Carmo & Flaherty Francis \(1992\)](#).

Definition A.9 (Riemannian Manifolds). A Riemannian metric on \mathcal{M} is a smooth symmetric covariant 2-tensor field on \mathcal{M} , which is positive definite at every point. A Riemannian manifold is a pair $\{\mathcal{M}, g\}$, where \mathcal{M} is a smooth manifold and g is a Riemannian metric.

As a basic fact in differential geometry, every smooth manifold is a Riemannian manifold (Do Carmo & Flaherty Francis, 1992, Proposition 2.10, Chatper 1). Therefore, in the following, we will alternatively use manifolds or Riemannian manifolds.

Definition A.10 (Pullback Metrics). Suppose \mathcal{M}, \mathcal{N} are smooth manifolds, g is a Riemannian metric on \mathcal{N} , and $f : \mathcal{M} \rightarrow \mathcal{N}$ is smooth. Then the pullback of a tensor field g by f is defined point-wisely,

$$(f^*g)_p(V_1, V_2) = g_{f(p)}(f_{*,p}(V_1), f_{*,p}(V_2)), \quad (40)$$

where p is an arbitrary point in \mathcal{M} , $f_{*,p}(\cdot)$ is the differential map of f at p , and V_1, V_2 are tangent vectors in $T_p\mathcal{M}$. If f^*g is positive definite, it is a Riemannian metric on \mathcal{M} , called the pullback metric defined by f .

Definition A.11 (Isometries). If $\{M, g\}$ and $\{\widetilde{M}, \widetilde{g}\}$ are both Riemannian manifolds, a smooth map $f : M \rightarrow \widetilde{M}$ is called a (Riemannian) isometry if it is a diffeomorphism that satisfies $f^*\widetilde{g} = g$.

If two manifolds are isometric, they can be viewed as equivalent. Riemannian operators in these two manifolds are closely related.

Definition A.12 (Bi-invariance). A Riemannian metric g over a Lie group $\{G, \odot\}$ is left-invariant, if for any $x, y \in G$ and $V_1, V_2 \in T_x G$,

$$g_y(V_1, V_2) = g_{L_x(y)}(L_{x*,y}(V_1), L_{x*,y}(V_2)), \quad (41)$$

where $L_x(y) = x \odot y$ is left translation, and $L_{x*,y}$ is the differential map of L_x at y . Right-invariance is defined similarly. A metric over a Lie group is bi-invariant, if it is both left and right invariant.

Bi-invariant metrics are the most convenient metrics on Lie, as they enjoy many excellent properties (Sternberg, 1999, Chatper V).

The exponential & logarithmic maps and parallel transportation are also crucial for Riemannian approaches in machine learning. To bypass the notation burdens caused by their definitions, we review the geometric reinterpretation of these operators, introduced in Pennec et al. (2006); Do Carmo & Flaherty Francis (1992). In detail, in a manifold \mathcal{M} , geodesics correspond to straight lines in the Euclidean space. A tangent vector $\vec{xy} \in T_x\mathcal{M}$ can be locally identified to a point y on the manifold by geodesic starting at x with initial velocity of \vec{xy} , i.e. $y = \text{Exp}_x(\vec{xy})$. On the other hand, logarithmic map is the inverse of exponential map, generating the initial velocity of the geodesic connecting x and y , i.e. $\vec{xy} = \text{Log}_x(y)$. These two operators generalize the idea of addition and subtraction in Euclidean space. For the parallel transportation $\Gamma_{x \rightarrow y}(V)$, it is a generalization of parallelly moving a vector along a curve in the Euclidean space. we summarize the reinterpretation in Table 4.

Table 4. Reinterpretation of Riemannian Operators.

Operations	Euclidean spaces	Riemannian manifolds
Straight Line	Straight Line	Geodesic
Subtraction	$\vec{xy} = y - x$	$\vec{xy} = \log_x(y)$
Addition	$y = x + \vec{xy}$	$y = \exp_x(\vec{xy})$
Parallelly Moving	$V \rightarrow V$	$\Gamma_{x \rightarrow y}(V)$

A.3. Geometry of the SPD Manifold

Although SPD matrices is a subset of the vector space $\mathbb{R}^{n(n+1)/2}$, applying the Euclidean structure directly to SPD matrices could be problematic both practically and theoretically, as demonstrated in (Arsigny et al., 2005; Pennec et al., 2006). The reason is that this subset does not form a linear subspace of $\mathbb{R}^{n(n+1)/2}$ and is actually a manifold (Arsigny et al., 2005). As mentioned before, there are many kinds of well-studied Riemannian metrics on the SPD manifold. Below, we will briefly review two related metrics, LEM (Arsigny et al., 2005) and LCM (Lin, 2019).

Matrix logarithm $\phi_{mln}(\cdot) : \mathcal{S}_{++}^n \rightarrow \mathcal{S}^n$ and $\phi_{cln}(\cdot) : \mathcal{S}_{++}^n \rightarrow \mathcal{L}^n$ are defined as,

$$\phi_{mln}(S) = U \ln(\Sigma) U^\top, \quad (42)$$

$$\phi_{cln}(S) = \varphi_{ln}(\mathcal{L}(S)), \quad (43)$$

where $S = U \Sigma U^\top$ is the eigendecomposition, $L = \mathcal{L}(S)$ is the Cholesky decomposition ($S = LL^\top$), $\varphi_{ln}(L) = \lfloor L \rfloor + \ln(\mathbb{D}(L))$ is a coordinate system from the \mathcal{L}_+^n manifold onto the Euclidean space \mathcal{L}^n (Lin, 2019), $\lfloor L \rfloor$ is the strictly lower triangular part of L , $\mathbb{D}(L)$ is the diagonal elements, and $\ln(\cdot)$ is the diagonal natural logarithm. We name ϕ_{cln} as Cholesky logarithm, since in the following proof we will rely on it many times. Note that topologically, $\mathcal{L}^n \simeq \mathcal{S}^n \simeq \mathbb{R}^{n(n+1)/2}$, since their metric topology all comes from the Euclidean metric tensor. Based on matrix logarithm, Arsigny et al. (2005) propose LEM by Lie group translation, while based on Cholesky logarithm, Lin (2019) proposes LCM, by an isometry between \mathcal{S}_{++}^n and \mathcal{L}_+^n . In the main paper, we argued that LEM and LCM are basically the same, in the sense of high-level mathematical abstraction.

The Riemannian metric and associated geodesic distance under the LEM are defined by:

$$g_S^{\text{LE}}(V_1, V_2) = g^E(\phi_{mln*}, S(V_1), \phi_{mln*}, S(V_2)), \quad (44)$$

$$d^{\text{LE}}(S_1, S_2) = \|\phi_{mln}(S_1) - \phi_{mln}(S_2)\|_F, \quad (45)$$

where $S \in \mathcal{S}_{++}^n$, $V_1, V_2 \in T_S \mathcal{S}_{++}^n$ are tangent vectors, $\phi_{mln*}(\cdot)$ is the differential map of matrix logarithm at S , g^E is the standard Euclidean metric tensor, and $\|\cdot\|_F$ is Frobenius norm. Note that since g^E is the same at every point, we simply omit the subscript. Besides, element-wise

and scalar multiplication are also induced by ϕ_{mln} :

$$S_1 \odot_{mln} S_2 = \phi_{mexp}(\phi_{mln}(S_1) + \phi_{mln}(S_2)), \quad (46)$$

$$\lambda \circledast_{mln} S = \phi_{mexp}(\lambda \phi_{mln}(S)), \quad (47)$$

where $\phi_{mexp}(X) = U \exp(\Sigma) U^\top$ is the matrix exponential. As is proven in Arsigny et al. (2005), $\{\mathcal{S}_{++}^n, \odot_{mln}\}$ and $\{\mathcal{S}_{++}^n, \circledast_{mln}, \circledast_{mln}\}$ form a Lie group and vector space, respectively. Besides, the metric g^{LE} defined on Lie group $\{\mathcal{S}_{++}^n, \odot_{mln}\}$ is bi-invariant.

The Riemannian metric and geodesic distance under LCM is

$$g_S^{\text{LC}}(V_1, V_2) = \tilde{g}_L(L(L^{-1}V_1 L^{-\top})_{\frac{1}{2}}, L(L^{-1}V_2 L^{-\top})_{\frac{1}{2}}), \quad (48)$$

$$d^{\text{LC}}(S_1, S_2) = \{\| \lfloor L_1 \rfloor - \lfloor L_2 \rfloor \|_{\text{F}}^2 + \|\ln(\mathbb{D}(L_1)) - \ln(\mathbb{D}(L_2))\|_{\text{F}}^2\}^{\frac{1}{2}}, \quad (49)$$

where $S \in \mathcal{S}_{++}^n$, $V_1, V_2 \in T_S \mathcal{S}_{++}^n$, $X_{\frac{1}{2}} = \lfloor X \rfloor + \mathbb{D}(X)/2$, and $\tilde{g}_L(\cdot, \cdot)$ is the Riemannian metric on \mathcal{L}_+^n , defined as

$$\begin{aligned} \tilde{g}_L(X, Y) &= g^{\text{E}}(\lfloor X \rfloor, \lfloor Y \rfloor) \\ &+ g^{\text{E}}(\mathbb{D}(L)^{-1}\mathbb{D}(X), \mathbb{D}(L)^{-1}\mathbb{D}(Y)). \end{aligned} \quad (50)$$

The group operation in Lin (2019) is defined as follows:

$$S_1 \odot_{cln} S_2 = \mathcal{L}^{-1}(\lfloor L_1 \rfloor + \lfloor L_2 \rfloor + \mathbb{D}(L_1)\mathbb{D}(L_2)), \quad (51)$$

where $\mathcal{L}^{-1}(\cdot)$ is the inverse map of Cholesky decomposition. $\{\mathcal{S}_{++}^n, \odot_{cln}\}$ is proven to be a Lie group (Lin, 2019). Similar with LEM, g^{LC} is bi-invariant.

A.4. Building Blocks in the SPDNet

The architecture of SPDNet (Huang & Van Gool, 2017) mimics the conventional densely connected feedforward network. It has three basic components, named BiMap, ReEig, and LogEig.

The BiMap (Bilinear Mapping) is a generalized version of conventional linear mapping, defined as

$$S^k = W^k S^{k-1} W^k, \text{ with } W^k \text{ semi-orthogonal.} \quad (52)$$

The ReEig (Eigenvalue Rectification) can be viewed as eigen-rectification, mimicking the ReLu-like nonlinear activation functions:

$$X^k = U^k \max(\Sigma^k, \epsilon I_n) U^{k\top}, \quad (53)$$

where $P^k = U^k \Sigma^k U^{k\top}$ is the eigendecomposition.

The LogEig layer projects SPD-valued data into the Euclidean space for further classification:

$$X^k = \phi_{mln}(X^{k-1}). \quad (54)$$

B. Proofs for the Lemmas, Propositions, Theorems, and Corollaries Stated in the Paper

Proof of Theorem 3.1. Recalling Definition A.11, to show the isometry, we need to find the pullback formulation.

Let us first deal with the LEM. Recalling Eq. 44, we can readily conclude that ϕ_{mlog} is an isometry from $\{\mathcal{S}_{++}^n, g^{\text{LE}}\}$ onto $\{\mathbb{R}^{n(n+1)/2}, g^{\text{E}}\}$.

Now, let us focus on LCM. By Eq. 48, $\{\mathcal{S}_{++}^n, g^{\text{LC}}\}$ is isometric to $\{\mathcal{L}_+^n, \tilde{g}\}$, with Cholesky decomposition \mathcal{L} as an isometry. This is exactly how LCM is derived (Lin, 2019). So, the key point lies in Cholesky metric \tilde{g} . Let us reveal why it is defined in this way. In fact, \tilde{g} is derived from g^{E} by φ_{ln} . Simple computations show that

$$\varphi_{ln*,L}(V) = \lfloor V \rfloor + \mathbb{D}^{-1}(L)\mathbb{D}(V), \quad (55)$$

where $V \in T_L \mathcal{L}_+^n$. By Eq. 55, Eq. 50 can be rewrote as

$$\tilde{g}_L(X, Y) = g^{\text{E}}(\varphi_{ln*,L}((X), \varphi_{ln*,L}((Y))). \quad (56)$$

Therefore, $\varphi_{ln} : \mathcal{L}_+^n \rightarrow \mathbb{R}^{n(n+1)/2}$ is an isometry. By transitivity, $\phi_{cln} : \mathcal{S}_{++}^n \rightarrow \mathbb{R}^{n(n+1)/2}$ is an isometry as well. \square

Proof of Lemma 4.1. First, let's focus on the case 1. Before starting, we point out that Eq. 4-Eq. 6 are indeed well-defined, which is easy to verify by the bijectivity of ϕ and the well-defined operations on \mathcal{Y} . More explicitly, the three maps should be expressed as the following,

$$\odot_\phi : \mathcal{X} \times \mathcal{X} \rightarrow \mathcal{X}, \quad (57)$$

$$\circledast_\phi : \mathbb{K} \times \mathcal{X} \rightarrow \mathcal{X}, \quad (58)$$

$$\langle \cdot, \cdot \rangle_\phi : \mathcal{X} \times \mathcal{X} \rightarrow \mathbb{K}. \quad (59)$$

In the following, we first show that $\{\mathcal{X}, \odot_\phi\}$ is an abelian group and then $\{\mathcal{X}, \odot_\phi, \circledast_\phi\}$ is a vector space over \mathbb{K} . Next, we proceed to verify $\{\mathcal{X}, \odot_\phi, \circledast_\phi, \langle \cdot, \cdot \rangle_\phi\}$ is an inner product space. Lastly, we will prove the completeness of $\{\mathcal{X}, \odot_\phi, \circledast_\phi, \langle \cdot, \cdot \rangle_\phi\}$.

Given arbitrary $x, x_1, x_2, x_3 \in \mathcal{X}$ and $k, l \in \mathbb{K}$, we have the following proof. Note that we would not emphasize the arbitrariness again in the following description.

Firstly, to prove a non-empty set endowed with an operation is an abelian group. We need to verify: 1). closure under this operation, 2). associativity and commutativity, 3). left identity element, 4). left invertibility.

For 1), it can be verified directly by the bijectivity of ϕ .

For 2), it can be guaranteed by the associativity and commu-

tativity of $\odot_{\mathcal{Y}}$,

$$\begin{aligned}
 (x_1 \odot_{\phi} x_2) \odot_{\phi} x_3 &= [\phi^{-1}(\phi(x_1) \odot_{\mathcal{Y}} \phi(x_2))] \odot_{\phi} x_3 \\
 &= \phi^{-1}((\phi(x_1) \odot_{\mathcal{Y}} \phi(x_2)) \odot_{\mathcal{Y}} \phi(x_3)) \\
 &= \phi^{-1}(\phi(x_1) \odot_{\mathcal{Y}} (\phi(x_2) \odot_{\mathcal{Y}} \phi(x_3))) \\
 &= x_1 \odot_{\phi} (x_2 \odot_{\phi} x_3)
 \end{aligned} \tag{60}$$

$$\begin{aligned}
 x_1 \odot_{\phi} x_2 &= \phi^{-1}(\phi(x_1) \odot_{\mathcal{Y}} \phi(x_2)) \\
 &= \phi^{-1}(\phi(x_2) \odot_{\mathcal{Y}} \phi(x_1)) \\
 &= x_2 \odot_{\phi} x_1
 \end{aligned} \tag{61}$$

For 3), denoting the neutral element in \mathcal{Y} as $\mathbb{1}_{\mathcal{Y}}$, we then have,

$$\begin{aligned}
 \phi^{-1}(\mathbb{1}_{\mathcal{Y}}) \odot_{\phi} x &= \phi^{-1}(\mathbb{1}_{\mathcal{Y}} \odot_{\mathcal{Y}} \phi(x)) \\
 &= \phi^{-1}(\phi(x)) \\
 &= x.
 \end{aligned} \tag{62}$$

For 4), denoting $y_{\odot_{\mathcal{Y}}}^{-1}$ as the inverse element of $y \in \mathcal{Y}$ and $x_{\odot_{\phi}}^{-1} = \phi^{-1}(\phi(x)_{\odot_{\mathcal{Y}}}^{-1})$, we have,

$$\begin{aligned}
 x_{\odot_{\phi}}^{-1} \odot_{\phi} x &= \phi^{-1}(\phi(x)_{\odot_{\mathcal{Y}}}^{-1} \odot_{\mathcal{Y}} \phi(x)) \\
 &= \phi^{-1}(\mathbb{1}_{\mathcal{Y}}) \\
 &= \mathbb{1}_{\mathcal{X}}
 \end{aligned} \tag{63}$$

So far, we prove that $\{\mathcal{X}, \odot_{\phi}\}$ is an abelian group. To show $\{\mathcal{X}, \odot_{\phi}, \circledast_{\phi}\}$ is a linear space, we only need to verify four laws about scalar product. we have the following equations to support our claim:

$$\begin{aligned}
 1 \circledast_{\phi} x &= \phi^{-1}(1 \circledast_{\mathcal{Y}} \phi(x)) \\
 &= \phi^{-1}(\phi(x)) \\
 &= x,
 \end{aligned} \tag{64}$$

$$\begin{aligned}
 k \circledast_{\phi} (x_1 \odot_{\phi} x_2) &= k \circledast_{\phi} [\phi^{-1}(\phi(x_1) \odot_{\mathcal{Y}} \phi(x_2))] \\
 &= \phi^{-1}(k \circledast_{\mathcal{Y}} [\phi(x_1) \odot_{\mathcal{Y}} \phi(x_2)]) \\
 &= \phi^{-1}([k \circledast_{\mathcal{Y}} \phi(x_1)] \odot_{\mathcal{Y}} [k \circledast_{\mathcal{Y}} \phi(x_2)]) \\
 &= (k \circledast_{\phi} x_1) \odot_{\phi} (k \circledast_{\phi} x_2),
 \end{aligned} \tag{65}$$

$$\begin{aligned}
 (k + l) \circledast_{\phi} x &= \phi^{-1}((k + l) \circledast_{\mathcal{Y}} \phi(x)) \\
 &= \phi^{-1}((k \circledast_{\mathcal{Y}} \phi(x)) \odot_{\mathcal{Y}} (l \circledast_{\mathcal{Y}} \phi(x))) \\
 &= (k \circledast_{\phi} x) \odot_{\phi} (l \circledast_{\phi} x),
 \end{aligned} \tag{66}$$

$$\begin{aligned}
 k \circledast_{\phi} (l \circledast_{\phi} x) &= k \circledast_{\phi} \phi^{-1}(l \circledast_{\mathcal{Y}} \phi(x)) \\
 &= \phi^{-1}(k \circledast_{\mathcal{Y}} (l \circledast_{\mathcal{Y}} \phi(x))) \\
 &= \phi^{-1}((kl) \circledast_{\mathcal{Y}} \phi(x)) \\
 &= (kl) \circledast_{\phi} x.
 \end{aligned} \tag{67}$$

Now, we see \mathcal{X} is a linear space. Next, we verify that $\langle \cdot, \cdot \rangle_{\phi}$ is an inner product. This means it should satisfy: a). positivity, b). definiteness, c). linearity in the first slot, and d). symmetry.

For a)-d), they all can be derived by the corresponding properties of inner product in \mathcal{Y} :

$$\langle x, x \rangle_{\phi} = \langle \phi(x), \phi(x) \rangle_{\mathcal{Y}} \geq 0, \tag{68}$$

$$\begin{aligned}
 \langle x, x \rangle_{\phi} = 0 &\iff \langle \phi(x), \phi(x) \rangle_{\mathcal{Y}} = 0, \\
 &\iff \phi(x) = \mathbb{1}_{\mathcal{Y}}, \\
 &\iff x = \mathbb{1}_{\mathcal{X}},
 \end{aligned} \tag{69}$$

$$\begin{aligned}
 \langle x_1 \odot_{\phi} x_3, x_2 \rangle_{\phi} &= \langle \phi(x_1) \odot_{\mathcal{Y}} \phi(x_3), \phi(x_2) \rangle_{\mathcal{Y}} \\
 &= \langle \phi(x_1), \phi(x_2) \rangle_{\mathcal{Y}} + \langle \phi(x_3), \phi(x_2) \rangle_{\mathcal{Y}} \\
 &= \langle x_1, x_2 \rangle_{\phi} + \langle x_3, x_2 \rangle_{\phi}
 \end{aligned} \tag{70}$$

$$\begin{aligned}
 \langle k \circledast_{\phi} x_1, x_2 \rangle_{\phi} &= \langle \phi^{-1}(k \circledast_{\mathcal{Y}} \phi(x_1)), x_2 \rangle_{\phi} \\
 &= \langle k \circledast_{\mathcal{Y}} \phi(x_1), \phi(x_2) \rangle_{\mathcal{Y}} \\
 &= k \langle \phi(x_1), \phi(x_2) \rangle_{\mathcal{Y}} \\
 &= k \langle x_1, x_2 \rangle_{\phi}
 \end{aligned} \tag{71}$$

$$\begin{aligned}
 \langle x_1, x_2 \rangle_{\phi} &= \langle \phi(x_1), \phi(x_2) \rangle_{\mathcal{Y}} \\
 &= \langle \phi(x_2), \phi(x_1) \rangle_{\mathcal{Y}} \\
 &= \langle x_2, x_1 \rangle_{\phi},
 \end{aligned} \tag{72}$$

Recall the above proof, we can find that ϕ is a linear isomorphism that could preserve the inner product and thus an isometry.

Last but not least, we verify \mathcal{X} is complete. Since \mathcal{Y} is complete and ϕ is an isometric bijection, therefore \mathcal{X} is complete as well.

Now, let us deal with case 2. We can see that ϕ is a group isomorphism and \mathcal{X} is a group. What's left is to verify the smoothness of the group operations. First, we present the multiplications and inverses more explicitly,

$$m_{\mathcal{Y}}(\cdot, \cdot) : \mathcal{Y} \times \mathcal{Y} \rightarrow \mathcal{Y}, \tag{73}$$

$$i_{\mathcal{Y}}(\cdot) : \mathcal{Y} \rightarrow \mathcal{Y}, \tag{74}$$

$$m_{\mathcal{X}}(\cdot, \cdot) : \mathcal{X} \times \mathcal{X} \rightarrow \mathcal{X}, \tag{75}$$

$$i_{\mathcal{X}}(\cdot) : \mathcal{X} \rightarrow \mathcal{X}, \tag{76}$$

where $m_{\mathcal{Y}}, i_{\mathcal{Y}}$ mean the multiplication and inverse in \mathcal{Y} , and $m_{\mathcal{X}}, i_{\mathcal{X}}$ mean the counterparts in \mathcal{X} . Recalling Eq. 4, we rewrite group operations as

$$m_{\mathcal{X}} = \phi^{-1} \circ m_{\mathcal{Y}} \circ (\phi \times \phi), \tag{77}$$

$$i_{\mathcal{X}} = \phi^{-1} \circ i_{\mathcal{Y}} \circ \phi, \tag{78}$$

where $\phi \times \phi$ means the Cartesian product of two maps. Since $m_{\mathcal{Y}}, i_{\mathcal{Y}}, \phi$ and ϕ^{-1} are all smooth, as the composition and Cartesian product of some smooth maps, $m_{\mathcal{X}}$ and $i_{\mathcal{X}}$ are therefore smooth, which means that \mathcal{X} is a Lie group. Considering ϕ is a diffeomorphism and a group isomorphism, it is, therefore, a Lie group isomorphism.

Lastly, let us deal with case 3. By the Definition 2.1 and Definition A.11, we can readily conclude that ϕ is a Riemannian isometry from $\{\mathcal{X}, g^{\phi}\}$ into $\{\mathcal{Y}, g^{\mathcal{Y}}\}$. \square

Proof of Theorem 4.2. This is just a special case of Lemma 4.1. With the global exponential & logarithmic maps, and parallel transportation in Euclidean space, and the properties of Riemannian isometry, Eq. 12-Eq. 14 can be derived.

Now we prove the bi-invariance. For any $P, Q \in \mathcal{S}_{++}^n$ and $V_1, V_2 \in T_p \mathcal{S}_{++}^n$, we make the following discussion. Denote the left translation by Y in \mathcal{S}^n as

$$m_Y : X \in \mathcal{S}^n \rightarrow Y + X. \quad (79)$$

By simple computation, $m_{Y,*}$ is the identity map at any point. Then the left translation L_Q by Q on $\{\mathcal{S}_{++}^n, \odot\}$ can be rewrote as

$$L_Q = \phi^{-1} \circ m_{\phi(Q)} \circ \phi. \quad (80)$$

By the chain rule of differential, we have

$$L_{Q*,P} = \phi_{*,\phi(Q)+\phi(P)}^{-1} m_{\phi(Q)*,\phi(P)} \phi_{*,P}, \quad (81)$$

$$= \phi_{*,\phi(Q)+\phi(P)}^{-1} \phi_{*,P} \quad (82)$$

Note that

$$\phi_{*,L_Q(P)} \phi_{*,\phi(Q)+\phi(P)}^{-1} = \mathbb{1} \quad (83)$$

Then we have the following equations,

$$\begin{aligned} & \langle L_{Q*,P} V_1, L_{Q*,P} V_2 \rangle_{L_Q(P)}, \\ &= \langle \phi_{*,L_Q(P)} L_{Q*,P} V_1, \phi_{*,L_Q(P)} L_{Q*,P} V_2 \rangle_I, \\ &= \langle \phi_{*,P} V_1, \phi_{*,P} V_2 \rangle_I, \\ &= \langle V_1, V_2 \rangle_P, \end{aligned} \quad (84)$$

\square

Proof of Proposition 4.4. Obviously, ϕ_{ma} is the inverse of ϕ_{mlog} . What followed is to verify the smoothness of ϕ_{mlog} and its inverse.

According to Theorem 8.9 in Magnus & Neudecker (2019), the map producing an eigenvalue or an eigenvector from a real symmetric matrix is C^∞ . Recalling ϕ_{mlog} and its inverse map ϕ_{ma} , it's obvious that they are comprised of arithmetic or composition of some smooth maps. Therefore, ϕ_{mlog} (ϕ_{ma}) is a diffeomorphism. \square

Proof of Corollary 4.6. This is a direct result of Theorem 4.2. \square

Proof of Proposition 4.8. The differentials of ϕ_{ma} and ϕ_{mlog} can be derived in exactly the same way. In the following, we only present the process of deriving the differential of ϕ_{mlog} .

First, Let us recall the differentials of eigenvalues and eigenvectors. Theorem 8.9 in Magnus & Neudecker (2019) offers their Euclidean differentials, which are the exact formulations for differentials under the canonical base on SPD manifolds. So, we can readily obtain the differentials of eigenvalues and eigenvectors as the following:

$$\sigma_{*,S}(V) = u^\top V u, \quad (85)$$

$$u_{*,S}(V) = (\sigma I - S)^+ V u, \quad (86)$$

where $Su = \sigma u$, $u^\top u = 1$, and $(\cdot)^+$ is the Moore–Penrose inverse.

By the RHS of Eq. 29, the differential map of ϕ_{mlog} is

$$\begin{aligned} \phi_{mlog*,S}(V) &= U_{*,S}(V) \log(\Sigma) U^\top + U(\log \Sigma)_{*,S}(V) U^\top \\ &\quad + U \log(\Sigma) U_{*,S}^\top(V) \\ &= Q + Q^\top + U^\top (\log \Sigma)_{*,S}(V) U, \end{aligned} \quad (87)$$

where $Q = U_{*,S}(V) \log(\Sigma) U^\top$.

For the differential of diagonal logarithm, it is

$$\log_{*,S} \Sigma = A \frac{1}{\Sigma} \Sigma_{*,S}, \quad (88)$$

where A is defined in Eq. 30.

Denote the eigenvectors and eigenvalues of $S = U \Sigma U^\top$ as $U = (u_1, \dots, u_n)$ and $\Sigma = \text{diag}(\sigma_1, \dots, \sigma_n)$. By Eq. 85–Eq. 88, the differential of ϕ_{mlog} can be obtained. \square

Proof of Proposition 4.9. Following the notations in the proposition, we make the following proof. By abuse of notation, in the following, we omit the wide tilde $\tilde{\cdot}$.

Now, we proceed to deal with the differential of ϕ_{ma} . We rewrite the formula of ϕ_{ma} as

$$\phi_{ma}(X) \quad (89)$$

$$= U \alpha(\Sigma) U^\top, \quad (90)$$

$$= U \text{diag}(e^{\ln^{a_1} \sigma_1}, \dots, e^{\ln^{a_n} \sigma_n}) U^\top, \quad (91)$$

$$= U \text{diag}\left(\sum_{k=0}^{\infty} \frac{(\ln^{a_1} \sigma_1)^k}{k!}, \dots, \sum_{k=0}^{\infty} \frac{(\ln^{a_n} \sigma_n)^k}{k!}\right) U^\top, \quad (92)$$

$$= U \left(\sum_{k=0}^{\infty} \frac{B\Sigma}{k!}\right) U^\top, \quad (93)$$

$$= \sum_{k=0}^{\infty} \frac{PX}{k!} \quad (94)$$

where $P = UBU^\top$, with U from eigendecomposition $X = U\Sigma U^\top$ and diagonal matrix $B = \text{diag}(\ln^{a_1}, \dots, \ln^{a_n})$. By the properties of normed vector algebras (Tu, 2011, Proposition 15.14, § 15.4), we can obtain the last equation. Then, we can compute the differential of ϕ_{ma} by curves. Given a curve c on \mathcal{S}^n starting at X with initial velocity $W \in T_X \mathcal{S}^n$, we have

$$\phi_{ma*,X}(W) = \frac{d}{dt} \Big|_{t=0} \phi_{ma} \circ c(t) \quad (95)$$

$$= \frac{d}{dt} \Big|_{t=0} \sum_{k=0}^{\infty} \frac{Pc(t)}{k!}. \quad (96)$$

By a term-by-term differentiation, we have

$$\begin{aligned} \phi_{ma*,X}(W) \\ = \sum_{k=1}^{\infty} \frac{1}{k!} \left(\sum_{l=0}^{k-1} (PX)^{k-l-1} \frac{d}{dt} \Big|_{t=0} (Pc)(PX)^l \right). \end{aligned} \quad (97)$$

By the chain rule, we have

$$\frac{d}{dt} \Big|_{t=0} (Pc) = P'(0)X + PV. \quad (98)$$

$P'(0)$ is obtained by

$$P'(0) = (UBU^\top)'(0), \quad (99)$$

$$= U'(0)BU^\top + UBU^\top'(0), \quad (100)$$

$$= D_U BU^\top + UBD_U^\top, \quad (101)$$

where D_U is derived from the differential of eigenvectors,

$$D_U = \begin{pmatrix} (\sigma_1 I - S)^+ V u_1 & \dots & (\sigma_n I - S)^+ V u_n \end{pmatrix}. \quad (102)$$

Applying Eq. 98, Eq. 101 and Eq. 102 into Eq. 97, we have the differential of ϕ_{ma} . \square

Proof of Proposition 5.1. Obviously, the metric space $\{\mathcal{S}_{++}^n, d^{\text{ALE}}\}$ is isometric to the space \mathcal{S}^n endowed with the standard Euclidean distance. Therefore, the weighted Fréchet mean of $\{S_i\}$ in \mathcal{S}_{++}^n corresponds to the weighted Fréchet mean of associated points $\{\phi_{mlog}(S_i)\}$ in \mathcal{S}^n . The weighted Fréchet means in Euclidean spaces are clearly the familiar weighted means. \square

Proof of Proposition 5.2. This is a direct corollary of Theorem 4.2. \square

Proof of Proposition 5.3. Following the notations in this proposition, we make the following proof. The LHS can be

rewritten as

$$(\text{FM}(S_1^\beta, \dots, S_m^\beta)) = \phi_{ma} \left(\sum_{i=1}^m \frac{1}{m} \beta \phi_{mlog}(S_i) \right), \quad (103)$$

$$= \phi_{ma} \left(\beta \sum_{i=1}^m \frac{1}{m} \phi_{mlog}(S_i) \right), \quad (104)$$

$$= [\phi_{ma} \left(\sum_{i=1}^m \frac{1}{m} \phi_{mlog}(S_i) \right)]^\beta, \quad (105)$$

$$= (\text{FM}(S_1, \dots, S_m))^\beta \quad (106)$$

\square

Proof of Proposition 5.4. Obviously, for a given SPD matrix S ,

$$\phi_{mlog}(RSR^\top) = R\phi_{mlog}(S)R^\top, \quad (107)$$

$$\phi_{mlog}(s^2 S) = U(\log(s^2 I) + \phi_{mlog}(\Sigma))U^\top, \quad (108)$$

where $S = U\Sigma U^\top$ is the eigendecomposition. With Eq. 107 and Eq. 108, we can obtain the results. \square

Proof of Proposition 7.1. Let's first review the update formulation in the RSGD (Bonnabel, 2013), which is, geometrically speaking, a natural generalization of Euclidean stochastic gradient descent. For a minimization parameter w on an n -dimensional smooth connected Riemannian manifold \mathcal{M} , we have the following update,

$$w^{(t+1)} = \text{Exp}_w(-\gamma^{(t)} \pi_{w^{(t)}}(\nabla_{w^{(t)}} L)), \quad (109)$$

where $\text{Exp}_w(\cdot) : T_w \mathcal{M} \rightarrow \mathcal{M}$ is the Riemannian exponential map, which maps a tangent vector at w back into the manifold \mathcal{M} , and $\pi_w(\cdot) : \mathbb{R}^n \rightarrow T_w \mathcal{M}$ is the projection operator, projecting an ambient Euclidean vector into the tangent space at w . In the case of the SPD manifold, $\forall S \in \mathcal{S}_{++}^n, \forall X \in \mathbb{R}^{n \times n}, \forall V \in \mathcal{S}^n$, the exponential map and projection operator is formulated as the following:

$$\pi_S(X) = S \frac{X + X^\top}{2} S, \quad (110)$$

$$\text{Exp}_S(V) = S^{1/2} \phi_{mexp}(S^{-1/2} V S^{-1/2}) S^{1/2}, \quad (111)$$

where $\phi_{mexp}(\cdot)$ is the matrix exponential. For more details about Eq. 110 and Eq. 111, please kindly refer to Yger (2013) and Amari (2016). Substitute Eq. 110 and Eq. 111 into Eq. 109, Eq. 32 can be immediately obtained. \square

Proof of Proposition 7.2. Without loss of generality, we focus on the equivalence between $b = B_{11}$ and $a = \alpha_{11}$. Let us denote $\log_e^{(\cdot)}$ as $\ln^{(\cdot)}$. Note that b is essentially expressed as $b = \ln^a$. Supposing $b^{(t)} = \ln^{a^{(t)}}$, then we have

$$\nabla_{a^{(t)}} L = \nabla_{b^{(t)}} L \frac{\partial \ln^a}{a} \Big|_{a^{(t)}} \quad (112)$$

$$= \nabla_{b^{(t)}} L \frac{1}{a^{(t)}}. \quad (113)$$

according to the update Eq. 32, then $\ln^{a^{(t+1)}}$ is

$$\begin{aligned}
 \ln^{a^{(t+1)}} &= \ln^{a^{(t)}} e^{-\gamma^{(t)} a^{(t)} \nabla_{a^{(t)}} L} \\
 &= \ln^{a^{(t)}} -\gamma^{(t)} a^{(t)} \nabla_{a^{(t)}} L \\
 &= \ln^{a^{(t)}} -\gamma^{(t)} a^{(t)} (\nabla_{b^{(t)}} L / a^t) \\
 &= \ln^{a^{(t)}} -\gamma^{(t)} \nabla_{b^{(t)}} L \\
 &= b^t - \gamma^{(t)} \nabla_{b^{(t)}} L.
 \end{aligned} \tag{114}$$

The last row is the exact updated formula of ESGD for b .

Therefore, supposing $b^{(0)} = \ln^{a^{(0)}}$, then the optimization results after the overall training are equivalent. \square

Proof of Proposition 7.3. Eq. 33 is the so-called Daleckii-Krein formula presented in Bhatia (2009, Page 60). Now let us focus on the gradient w.r.t A . Differentiating both sides of Eq. 30:

$$dX = (*) + U dA \odot \log(\Sigma) U^T, \tag{115}$$

where $(*)$ means other parts related to dU and $d\Sigma$. According to the invariance of first-order differential form, we have,

$$\begin{aligned}
 \nabla_X L : dX \\
 = \nabla_S L : dS + \nabla_X L : (U dA \odot \log(\Sigma) U^T) \tag{116}
 \end{aligned}$$

$$= \nabla_S L : dS + [U^\top (\nabla_X L) U] \odot \log(\Sigma) : dA, \tag{117}$$

Where $A : B = \text{tr}(A^\top B)$ is the Euclidean Frobenius inner product. From the second term on the RHS of Eq. 117, we can obtain the gradient w.r.t A . \square

C. Details on the Datasets

HDM05. This dataset is comprised of motion capture data (MoCap) covering 130 action classes. Each data point is a sequence of frames of 31 3D coordinates. After vectorization, each sequence can be represented by a 93×93 temporal covariance matrix. For a fair comparison, we exploit the pre-processed 93×93 covariance features released by Brooks et al. (2019a), which trims the dataset down to 2086 points scattered throughout 117 classes by removing some under-represented classes. Following the settings in Brooks et al. (2019a), we split the dataset into 50% for training and 50% for testing.

FPHA. It includes 1,175 clips of 45 different action categories. Each frame is represented by 21 3D coordinates. Similarly, each sequence can be modelled by a 63×63 covariance matrix. For a fair comparison, we follow the experimental protocol in Garcia-Hernando et al. (2018), where 600 sequences are used for training and 575 sequences are used for testing.

AFEW. It consists of 7 kinds of emotions with 773 samples for training and 383 samples for validation. We use the released pre-trained FAN (Meng et al., 2019) to extract deep features and establish a 512×512 temporal covariance matrix for each video.

D. Additional Experiments and Explanations

D.1. Explanations for Nonlinear Mechanism in DIV

In the main paper, we mentioned that there is an underlying nonlinear scaling mechanism in the update of DIV. Without loss of generality, let us focus on one scalar parameter b in Eq. 31. The ultimate factor multiplied by the plain logarithm is $1/b$. Therefore, the change of the multiplier after the update would be

$$1/(b - \Delta) - 1/b = \Delta/[(b - \Delta)b]. \tag{118}$$

Eq. 118 will scale the original Δ to some extent. This scaling mechanism might undermine the robustness of the ALog layer.

D.2. Experiments on the SPDNetBN

In the main paper, we observed that among all three kinds of implementation of ALog, the most robust performance is achieved by MUL. So we exploit MUL to carry out further experiments on the SPDNetBN (Brooks et al., 2019a). In the following, we simply call SPDNetBN-ALog-MUL as SPDNetBN-ALog, where the LogEig layer is substituted by our ALog layer. Our experiments on three datasets show that SPDNetBN is similar to SPDNetBN-ALog. This could be attributed to the inconsistency of Riemannian metrics. The RBN in SPDNetBN is based on AIM, while the metric behind our ALog is ALEM. Therefore, it is not very reasonable to apply our ALog to AIM-based RBN. However, it does not undermine the effectiveness of our ALog. Instead, if one plans to apply our ALog to RBN, the RBN should be rebuilt based on ALEM. This clearly goes beyond the topics of this paper. We leave this for future work.